Alaska Department of Transportation & Public Facilities
Alaska University Transportation Center

Estimating Future Flood Frequency and Magnitude in Basins Affected by Glacier Wastage

Anna Liljedahl
Water and Environmental Research Center and International Arctic Research Center, University of Alaska Fairbanks

Contributing authors:

Matvey Debolskiy and Emily Youcha
Water and Environmental Research Center
University of Alaska Fairbanks

Anthony Arendt, Jennifer Davis, Regine Hock and Aurora Roth
Geophysical Institute
University of Alaska Fairbanks

Gabriel Wolken
Department of Natural Resources, Division of Geological and Geophysical Surveys

Jing Zhang
North Carolina A&T State University

March 2015

Alaska University Transportation Center
Duckering Building Room 245
P.O. Box 755900
Fairbanks, AK 99775-5900

Alaska Department of Transportation
Research, Development, and Technology Transfer
2301 Peger Road
Fairbanks, AK 99709-5399

INE/ AUTC 15.04

4000(119)

REPORT DOCUMENTATION PAGE

Form approved OMB No.

1. AGENCY USE ONLY (LEAVE BLANK)	2. REPORT DATE	3. REPORT TYPE AND DATES COVERED
4000(119)	March 2015	Final Report Sep 2012-2014

4. TITLE AND SUBTITLE
Estimating Future Flood Frequency and Magnitude in Basins Affected by Glacier Wastage

5. FUNDING NUMBERS
Alaska DOT&PF: T2-12-11
AUTC: S16806

6. AUTHOR(S)
Anna Liljedahl - Water and Environmental Research Center and International Arctic Research Center, University of Alaska Fairbanks

Contributing authors:
Matvey Debolskiy, Emily Youcha -Water and Environmental Research Center, University of Alaska Fairbanks
Anthony Arendt, Jennifer Davis, Regine Hock, Aurora Roth - Geophysical Institute University of Alaska Fairbanks
Gabriel Wolken - Department of Natural Resources, Division of Geological and Geophysical Surveys
Jing Zhang - North Carolina A&T State University

7. PERFORMING ORGANIZATION NAME(S) AND ADDRESS(ES)
Alaska University Transportation Center
University of Alaska Fairbanks
Duckering Building Room 245
P.O. Box 755900
Fairbanks, AK 99775-5900

8. PERFORMING ORGANIZATION REPORT NUMBER
INE/AUTC 15.04

9. SPONSORING/MONITORING AGENCY NAME(S) AND ADDRESS(ES)
State of Alaska, Alaska Dept. of Transportation and Public Facilities
Research and Technology Transfer
2301 Peger Rd
Fairbanks, AK 99709-5399

10. SPONSORING/MONITORING AGENCY REPORT NUMBER
4000(119)

11. SUPPLENMENTARY NOTES
Performed in cooperation with …..

12a. DISTRIBUTION / AVAILABILITY STATEMENT
No restrictions

12b. DISTRIBUTION CODE

13. ABSTRACT (Maximum 200 words)
We present field measurements of meteorology, hydrology and glaciers and long-term modeled projections of glacier mass balance and stream flow informed by downscaled climate simulations. The study basins include Valdez Glacier Stream (342 km^2), Jarvis Creek (634 km^2) and Phelan Creek (32 km^2), Alaska, that represent distinctly different climates and glacier coverage. At Phelan Cr., the decadal-averaged peak annual mean daily runoff was projected to increase 114 % from 14 (2000-2010) to 30 cms (2090-2099) with an 87 % increase by mid-century (2050-2059). At Jarvis, the decadal-averaged peak annual mean daily runoff was projected to decrease 14 % from 24 (2000-2010) to 21 cms (2066-2075), while the glacier contribution increased (from 37 % to 43 %). However, at Jarvis Cr., the flow at the 1% exceedance probability level was projected largest (~30 cms) during the mid-century time period (2035-2050). The highest flood events tended to have less glacier contribution, indicating that rainfall or snowmelt generated events may have a greater influence than glacier melt during peak flows (only Jarvis analyzed). The differing trends in projected runoff between the Jarvis and Phelan Cr. may be attributed to the differing climate forcing and glacier coverage representation, i.e. dynamic and static for Jarvis and Phelan Cr., respectively.

14- KEYWORDS :
Runoff(Jbhp), Glacier(Jbhyjjp), Forecasting (Epdmf)

15. NUMBER OF PAGES

16. PRICE CODE
N/A

17. SECURITY CLASSIFICATION OF REPORT	18. SECURITY CLASSIFICATION OF THIS PAGE	19. SECURITY CLASSIFICATION OF ABSTRACT	20. LIMITATION OF ABSTRACT
Unclassified	Unclassified	Unclassified	N/A

SI* (MODERN METRIC) CONVERSION FACTORS

APPROXIMATE CONVERSIONS TO SI UNITS

Symbol	When You Know	Multiply By	To Find	Symbol
		LENGTH		
in	inches	25.4	millimeters	mm
ft	feet	0.305	meters	m
yd	yards	0.914	meters	m
mi	miles	1.61	kilometers	km
		AREA		
in^2	square inches	645.2	square millimeters	mm^2
ft^2	square feet	0.093	square meters	m^2
yd^2	square yard	0.836	square meters	m^2
ac	acres	0.405	hectares	ha
mi^2	square miles	2.59	square kilometers	km^2
		VOLUME		
fl oz	fluid ounces	29.57	milliliters	mL
gal	gallons	3.785	liters	L
ft^3	cubic feet	0.028	cubic meters	m^3
yd^3	cubic yards	0.765	cubic meters	m^3
		NOTE: volumes greater than 1000 L shall be shown in m^3		
		MASS		
oz	ounces	28.35	grams	g
lb	pounds	0.454	kilograms	kg
T	short tons (2000 lb)	0.907	megagrams (or "metric ton")	Mg (or "t")
		TEMPERATURE (exact degrees)		
^oF	Fahrenheit	5 (F-32)/9 or (F-32)/1.8	Celsius	^oC
		ILLUMINATION		
fc	foot-candles	10.76	lux	lx
fl	foot-Lamberts	3.426	$candela/m^2$	cd/m^2
		FORCE and PRESSURE or STRESS		
lbf	poundforce	4.45	newtons	N
lbf/in^2	poundforce per square inch	6.89	kilopascals	kPa

APPROXIMATE CONVERSIONS FROM SI UNITS

Symbol	When You Know	Multiply By	To Find	Symbol
		LENGTH		
mm	millimeters	0.039	inches	in
m	meters	3.28	feet	ft
m	meters	1.09	yards	yd
km	kilometers	0.621	miles	mi
		AREA		
mm^2	square millimeters	0.0016	square inches	in^2
m^2	square meters	10.764	square feet	ft^2
m^2	square meters	1.195	square yards	yd^2
ha	hectares	2.47	acres	ac
km^2	square kilometers	0.386	square miles	mi^2
		VOLUME		
mL	milliliters	0.034	fluid ounces	fl oz
L	liters	0.264	gallons	gal
m^3	cubic meters	35.314	cubic feet	ft^3
m^3	cubic meters	1.307	cubic yards	yd^3
		MASS		
g	grams	0.035	ounces	oz
kg	kilograms	2.202	pounds	lb
Mg (or "t")	megagrams (or "metric ton")	1.103	short tons (2000 lb)	T
		TEMPERATURE (exact degrees)		
^oC	Celsius	1.8C+32	Fahrenheit	^oF
		ILLUMINATION		
lx	lux	0.0929	foot-candles	fc
cd/m^2	$candela/m^2$	0.2919	foot-Lamberts	fl
		FORCE and PRESSURE or STRESS		
N	newtons	0.225	poundforce	lbf
kPa	kilopascals	0.145	poundforce per square inch	lbf/in^2

*SI is the symbol for the International System of Units. Appropriate rounding should be made to comply with Section 4 of ASTM E380.
(Revised March 2003)

ACKNOWLEDGEMENTS / CREDITS

The development of MDSS concepts and the functional prototype is a team effort involving several U.S. national laboratories. The current MDSS development team at NCAR consists of several scientists and software engineers including Mike Chapman, Jim Cowie, Seth Linden, Gerry Weiner, Paddy MacCarthy, Crystal Burghardt, and Amanda Anderson.

Summary

The report presents field measurements of meteorology, hydrology and glaciers and long-term modeled projections of glacier mass balance and stream flow informed by downscaled climate simulations. The study basins in Alaska include Valdez Glacier Stream (342 km^2), Jarvis Creek (634 km^2) and Phelan Creek (32 km^2), which represents distinctly different climates and glacier coverage. Jarvis Cr. and Phelan Cr. experiences a sub-Arctic continental climate with semi-arid lowland precipitation (~ 140 mm rainfall and ~90 mm SWE at Delta Junction, 386 masl), while Valdez Glacier Stream is located in a maritime climate with high rain- and snowfall (~ 1800 mm yr^{-1} at 7 masl, Valdez). Glacier coverage amongst the three basins range from (<5 %) Jarvis Cr. to 58 % (Valdez Glacier Stream) with glacier covering 50 % of Phelan Cr. watershed.

Our field measurements in Jarvis Cr. and Valdez Glacier Stream, both with no previous or limited observations of runoff and glacier mass balance measurements, show that peak flows are typically concentrated to rain events and, in 2013, which experienced an unusually late melt in Interior Alaska, also early season snowmelt. Flow is year-round in the Jarvis Cr., although the winter baseflow (1 to 4 cms) rarely reach the Richardson Hwy Bridge due to extensive aufeis formation. Highest summer baseflow in Jarvis Cr. is in mid/late summer months, which also present the warmest temperatures at the glacier. In maritime Alaska (Valdez Glacier Stream), flow ceases completely in winter. Like Jarvis, high discharge events in Valdez Glacier Stream are linked to air temperature (snowmelt) and rainfall events during early and late summer, respectively. Specific total runoff in the 2012-2013 hydrologic year for the two basins were estimated to 200 mm (Jarvis Cr) and 3419 mm (Valdez Glacier Stream), which represents about 87 and 190 % of the total annual lowland precipitation, respectively. Glacier mass balance, which was measured via individual stakes, ranged from ~2 m (~1750 masl) to ~5.5 m (~1250 masl) of water equivalent at Jarvis Glacier, during 2011-2014. At the Valdez Glacier the total annual melt ranged from ~1 m (~1250 masl) to ~6 m (~75 masl) in 2013. Phelan Cr. has been extensively monitored by USGS.

Model projections of future runoff present increases in peak annual mean daily runoff at Phelan Cr., while Jarvis Cr. runoff saw a steady decrease in the decadal-averaged peak annual mean daily runoff. Projected precipitation was set unchanged in the Phelan Cr. simulations. The downscaled climate simulations that forced the hydrology/glacier modeling in Jarvis Cr. retained the average annual precipitation through a majority of the future years but suggested a 9 % decrease by late-century. In the simulations of the Jarvis Cr., the glacier was allowed to retreat as it melted, while Gulkana Glacier, Phelan Cr., was described a static glacier coverage. At Phelan Cr., the decadal-averaged peak annual mean daily runoff increased on average 114 % from 14 (2000-2010) to 30 cms (2090-2099) with a 87 % increase by mid-century (2050-2059, 27 cms). At Jarvis, the decadal-averaged peak annual mean daily runoff was projected to decrease (14 %) from 24 (2000-2010) to 21 cms (2066-2075), while the glacier contribution increased (from 37 % to 43 %, respectively). However, at Jarvis Cr., the flow at the 1% exceedance probability level was projected largest (~30 cms) during the mid-century time period (2035-2050). The highest flood events tended to have less glacier contribution, indicating that rainfall or snowmelt generated events may have a greater influence than glacier melt during peak flows (only Jarvis analyzed). We did not perform a partial duration flood analysis to assess whether floods events were increasing in number. The differing trajectories of long-term runoff projections at Phelan and Jarvis Creek's suggest that it is crucial to account for glacier retreat as a negative feedback runoff projections and/or that watersheds with small glacier coverage (~5 %) will, unlike high-glacier coverage basins, experience a future reduction in decadal-averaged peak annual mean daily runoff.

Content

Summary 2

Introduction 4

Site description 4
- Jarvis Cr. 5
- Valdez Glacier Stream 6
- Phelan Cr. 7

Results
- Jarvis Cr.
  - Meteorology 8
  - Snow accumulation 12
  - Glacier melt 12
  - Stream water levels 13
  - Runoff 13
  - Climate projections 16
  - Flood frequency analysis 18
- Valdez Glacier Stream
  - Meteorology 22
  - Lake water levels 26
  - Runoff 27
  - Temperature Index Modeling 29
- Phelan Cr.
  - Temperature Index Modeling 31
  - Flood frequency analysis 33

Acknowledgements 36

References 37

1. Introduction

Infrastructure, such as bridge crossings, requires informed structural designs in order to be effective and reliable for decades. A typical bridge is intended to operate for 75 years or more, a period of time that is anticipated to exhibit a warming climate and consequently, hydrologic changes. An understanding of present and future possible hydrologic conditions is necessary to avoid damage to critical infrastructure and costly disruptions to Alaska's transportation network.

Several major roads in Alaska cross streams that receive runoff from glacierized basins. Projections of glacier wastage under a warming climate show initial increases in glacier runoff (Hock et al. 2005; Radic and Hock, 2011), which can be substantial and exceed all other runoff components in a watershed (Adalgeirsdottir et al. 2006). Accordingly, flood events may become more frequent and more severe. Changes in the proportion of streamflow derived from glacial runoff will affect physical properties of streams such as overflow and stream reorganization (Hood and Berner 2009), which in turn, could have significant impacts on Alaska's infrastructure.

Engineering design criteria continue to rely heavily on the assumption that historical hydrologic conditions will persist. The validity of this claim for Alaska is weak, given the multitude of scientific literature that predicts altered hydroclimatology in coming decades. Efforts in assessing the impacts of climate variability and change on flood frequency and magnitude in Alaska have included statistical techniques confirming the importance of the Pacific Decadal Oscillation (Neal et al. 2002, Hodgkins 2009) and highlighted the constraints of limited runoff records in identifying trends (Tidwell 2010). An application of a physically-based hydrologic model, which is first validated in order to quantify its uncertainty, has the potential to extend statistical analyses into the future and ultimately inform management decisions.

The limited road network of Alaska is not only distributed across an enormous area but also over a multitude of climate regimes. Accordingly we expect a broad range of hydrologic responses to anticipated climate warming, each requiring different solutions in order to adequately manage risk and balance construction, maintenance and flood damage costs.

2. Site description

The study basins included Jarvis Creek (634 km2), Valdez Glacier Stream (342 km^2) and Phelan Creek (32 km^2). The watersheds represent distinctly different climates and glacier coverage (Table 1) and therefore, contrasting hydrologic systems. Jarvis Cr. (Delta Junction) experiences a sub-Arctic continental climate with potential evapotranspiration (Patric and Black, 1968) in summer exceeding typical summer rainfall. The Valdez Glacier Stream watershed, which is heavily glacierized and located in a maritime climate with high rain- and snowfall, has a lower potential evapotranspiration than rainfall. Jarvis Cr. has runoff throughout the year that is partly stored as aufeis in winter, while flow in the Valdez Glacier Stream ceases completely. Glacier and hydrological monitoring have been supported at Phelan Cr. (Gulkana Glacier) since the mid 1960's, while both Jarvis Cr. and the Valdez Glacier Stream have at best, received sporadic runoff measurements several decades ago (reference for Jarvis here).

Table 1. *Mean annual air temperature (MAAT), mean annual precipitation (MAP), mean air temperature (MAT) in January and July and elevation of longer-term (1970-2000) meteorological stations located near the study basins (Shulski and Wendler, 2007).*

NWS station	***MAAT (°C)***	***MAP (mm)***	***Jan. MAT (°C)***	***Jul. MAT (°C)***	***Elevation (masl)***	***Glaciated area (%)***
Delta Junction	-2.9	303	-23.1	21.3	386	<5 (JCr), 50 (PCr)
Valdez	3.5	1712	-5.9	16.8	7	58

2.1 Jarvis Creek

Jarvis Cr. serves as a proxy watershed of Interior Alaska basins that drain the north slopes of the Alaska Range (Fig. 1). Like many of the Tanana River sub-basins, Jarvis C. includes a semi-dry climate, high mountains (< 3000 m), glaciers and permafrost. Rivers that drain the north facing slopes of the Alaska Range are perched on top of relatively impermeable till that, in turn, overlay highly permeable outwash gravel. Once the rivers leave the mountains and exit the moraine, the streams loose significant amounts of water to the underlying aquifers. Creek beds of non-glacierized streams are typically dry for a majority of the summer, unlike the glacier fed streams that show continuous summer flow. Jarvis Cr. watershed represent the only glacier monitoring program that is located on the north side of the Alaska Range. The large orographic effects of the Alaska Range presents a contrasting environment in Jarvis compared to other Alaska Range glacier monitoring programs.

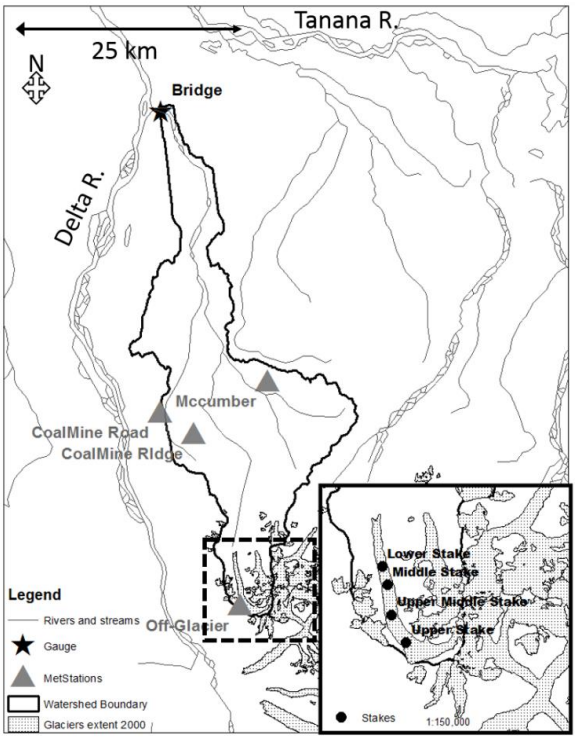

Figure 1. *Jarvis Cr. watershed boundary with the location of the Bridge runoff measurement site (star) and meteorological stations (triangles). The National Weather Service operated meteorological station is located about 5 km southeast of the runoff monitoring site. Glacier extent as of year 2000 and the mass balance stake locations are presented in the insert.*

Vegetation in the Jarvis Creek watershed range from bare rock and glaciers to alpine tundra, dense tall shrubs and willows to black spruce and deciduous forest. Discontinuous permafrost is found throughout the basin with active layers as shallow as ~0.5 m. Silt or till cover the top mineral soil horizon apart from the steepest mountain slopes. Small lakes are abundant on the moraine and the lowlands are a mosaic of burns of differing ages.

2.2 Valdez Glacier Stream

The Valdez catchment resides in a coastal maritime climate, with an average annual temperature of 3.5 ^{o}C, and an average annual precipitation of 1712 mm (NWS station in Valdez). The Valdez Glacier stream drains a 342 km^2 basin of which 43 % is covered by glaciers such as the 138 km^2 Valdez Glacier (Fig. 2). Between year 1950 to 2004 the Valdez Glacier retreated with an average mass balance of -1.37 ± 0.11 m yr^{-1} (Arendt et al., 2006).

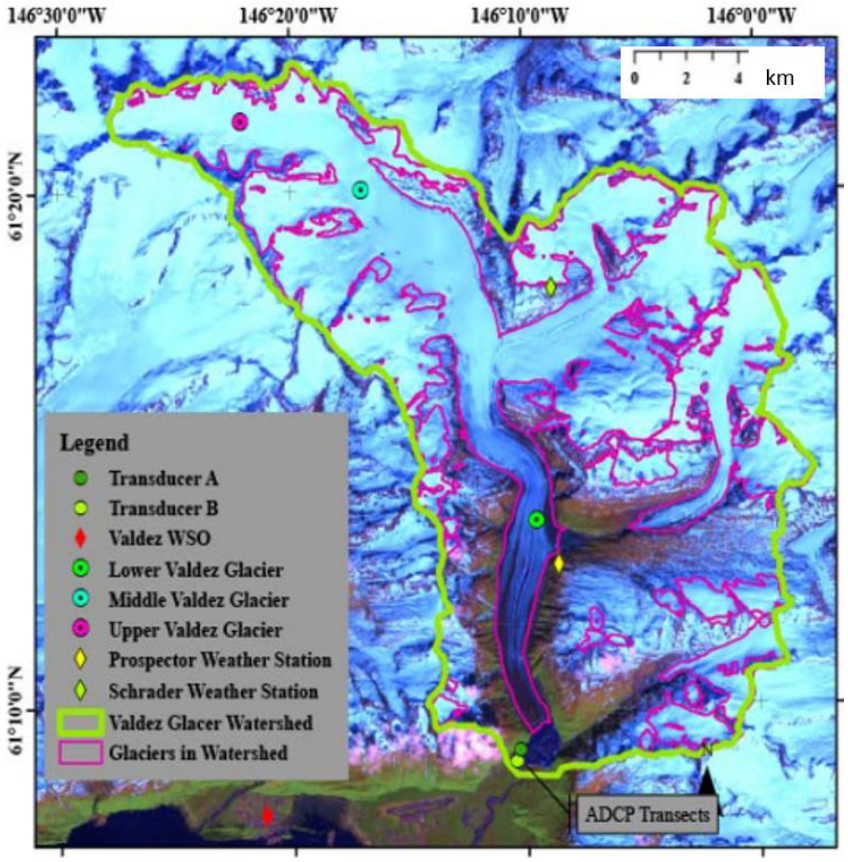

Figure 2. *Valdez Glacier Stream watershed boundary (green line) with the location of the runoff ("ADCP Transects") and water level ("Transducer A and B") measurement sites, meteorological stations including the National Weather Service station in Valdez ("Valdez WSO").*

The glacier retreat caused the formation of a 2 km^2 proglacial, moraine-dammed lake, which captures glacial runoff from Valdez and other glaciers in the catchment, as well as icebergs from calving events at the terminus of Valdez Glacier. The proglacial lake is drained via a braided stream network that flows adjacent to a gravel road, several recreational areas, the Valdez landfill, and lastly under Richardson Highway before entering Prince William Sound. The proglacial area consists primarily of glacial outwash (coarsely sorted sand and gravel with abundant silt. Shrub

vegetation covers portions of the proglacial area, while less recently disturbed areas are covered by deciduous forest. Shrubs flank the margins of the glacier up to 750 m, above which is alpine tundra or exposed bedrock. A marginal lake forms each summer on the eastern side of the lower ablation area (east of the Prospector/lower glacier weather station), filled by meltwater from an unnamed glacier. Aerial surveys and satellite data show that the lake drains every season, but the timing of the drainage event is currently unknown.

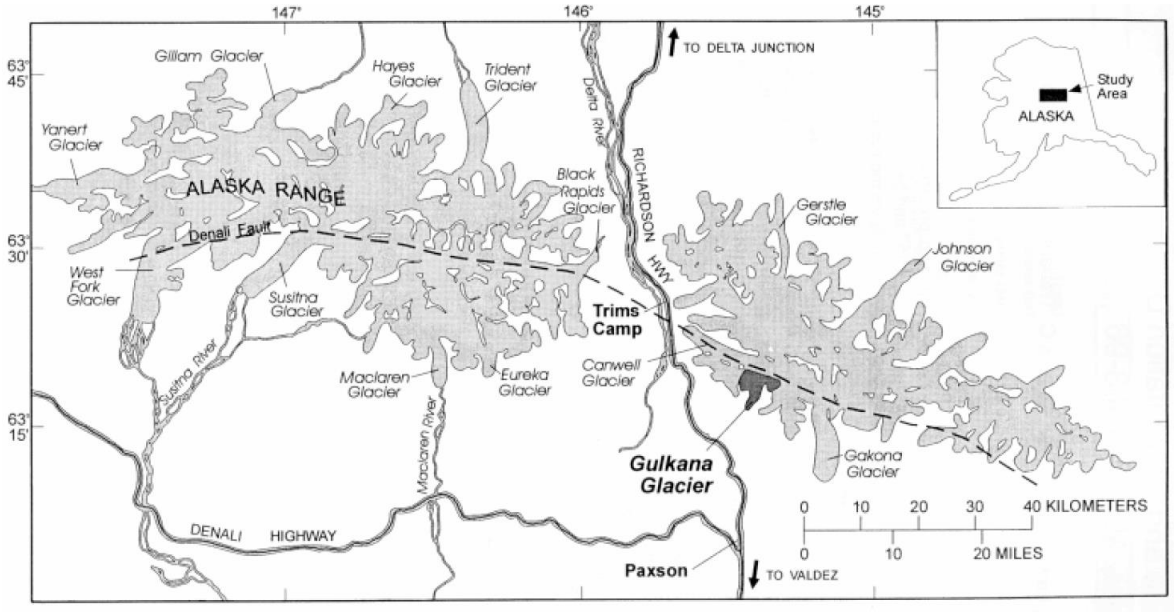

Figure 3. *Gulkana Glacier and Phelan Cr. watershed. Phelan Cr. drains the southern slopes of the Alaska Range. It is located about 30 km south of Jarvis Cr., which drains the north slopes of the Alaska Range.*

2.3 Phelan Creek

Phelan Cr. (32 km^2) is located about 30 km from the headwaters of Jarvis Cr. and the two drain the southern and northern slopes of the Alaska Range, respectively. Gulkana Glacier, Phelan Cr., is a long-term USGS glacier mass balance monitoring site. Since 1967, the glacier has lost a total of 25 m of water equivalent, while runoff has marginally increased (O'Neel et al. 2014). Thanks to the long-term dataset, a positive statistically significant correlation has also been established between summer glacier mass balance and runoff (O'Neel et al. 2014). On average, annual runoff from Phelan Cr. is estimated to contain less than 20% glacier meltwater, which is still larger than a maritime location (O'Neel et al. 2014).

3. Results

3.1 Jarvis Creek

3.1.1 Meteorology, Jarvis Cr.

Meteorological measurements were distributed across the Jarvis Cr. watershed to complement the existing National Weather Service station near the town of Delta Junction (Allen Army Airfield) to include McCumber, Coal Mine Road, Coal Mine Ridge and Off-Glacier meteorological stations (Fig. 1, Table 2). Meteorological measurements included air temperature and relative humidity (Hobo U23 with radiation shield, Onset) and rainfall (Hobo RG3, Onset). Precipitation buckets were removed in winter and installed in late March/early April. Rainfall was defined as recorded precipitation when air temperature exceeded −1 °C.

Table 2. *Location of meteorological and hydrological stations, Jarvis Cr.*

Site name	***Variable***	***Vegetation***	***X***	***Y***	***Elev. (masl)***
Delta Junction[1]	Meteorology	n/a	562466	7097125	389
McCumber	Meteorology	Tundra	571534	7066195	890
Coal Mine Road	Meteorology	Coniferous	558145	7063822	840
Coal Mine Ridge	Meteorology	Tundra	561974	7060795	1021
Off-glacier	Meteorology	Rock	565441	7039479	1650
Bridge	Runoff, stream water level	Coniferous/ deciduous	562243	7100272	358

[1] National Weather Service

[2] Tag-line

The largest variation in mean monthly air temperatures was observed at the lowest site (Delta Junction, −22 °C to 16 °C in 2012-2013), while the highest-elevated site recorded the least variation (Off-Glacier, −17 °C to 8 °C in 2012-2012 and −13 to 6 ºC in 2013-2014) (Table 3). June and July were the overall warmest months at all stations in 2013 and 2014, respectively, while the coldest month was represented by either November or December. Mean annual air temperature was coldest at the Off-Glacier (−6.2 ºC and −4.5 ºC) and warmest at the Coal Mine Road site (−2.8 °C and −0.2 ºC) in both years.

Mean daily air temperature throughout the year was most extreme at the lowland site (Delta Junction), with mean daily air temperatures ranging from – 43 °C to 24 °C in 2012-2013 with less extreme temperatures in 2013-2014 (Fig. 4). The lowest range in min/max mean daily air temperature was at the Off-glacier site (– 35 °C to 16 °C in 2012-2013). Above freezing air temperatures were recorded several times in mid-winter at the Coal Mine Ridge, while the temperatures remained below freezing at both Delta Junction and up at the glacier in 2012-2013. In 2014, however, air temperatures remained above freezing consistently for about a week in late January at the Coal Mine Ridge site with above 0ºC mean daily temperatures also observed at the Off-Glacier site. This was a very unusual warm late-January event that partially melted the snow pack and caused flow at the Richardson HWY bridge.

Table 3. *Mean monthly air temperatures during hydrologic year 2012-2013 and 2013-2014, Jarvis Cr.*

	2012			2013									
	Oct	**Nov**	**Dec**	**Jan**	**Feb**	**Mar**	**Apr**	**May**	**Jun**	**Jul**	**Aug**	**Sep**	*Mean*
Delta Junction	-6.0	-21.4	-22.1	-17.0	-15.0	-13.3	-9.7	4.5	16.3	15.7	12.0	2.0	*-4.4*
McCumber	-7.8	-17.3	-17.3	-12.4	-10.4	-12.1	-11.4	1.6	13.9	12.6	10.9	3.3	*-4.0*
Coal Mine Road	-6.6	-16.9	-16.3	-12.1	-9.6	-12.1	-9.8	3.2	15.3	13.6	12.0	4.0	*-2.8*
Coal Mine Ridge	-6.6	-16.7	-15.5	-11.1	-9.4	-11.4	-11.0	0.9	13.8	12.3	11.2	2.8	*-3.4*
Off-glacier	-9.1	-15.6	-15.8	-17.0	-15.0	-13.3	-14.3	-2.8	7.7	6.9	6.2	-1.8	*-6.2*

	2013			2014									
	Oct	**Nov**	**Dec**	**Jan**	**Feb**	**Mar**	**Apr**	**May**	**Jun**	**Jul**	**Aug**	**Sep**	*Mean*
Delta Junction	2.9	-14.2	-19.2	-9.1	-17.0	-8.3	0.8	9.6	12.4	14.7	13.5	7.1	*-0.6*
McCumber	1.6	-13.1	-13.9	-3.8	-14.9	-10.2	-1.5	6.3	8.9	11.0	9.9	7.3	*-1.0*
Coal Mine Road	1.8	-12.0	-13.0	-2.4	-13.6	-8.2	0.2	7.3	9.5	11.9	10.6	5.4	*-0.2*
Coal Mine Ridge	1.3	-11.3	-11.8	-2.5	-12.0	-8.9	-1.6	6.0	8.1	10.4	9.8	4.0	*-0.7*
Off-glacier	-5.0	-12.5	-13.2	-8.2	-12.0	-11.1	-3.8	0.4	2.4	5.7	4.4	-0.4	*-4.5*

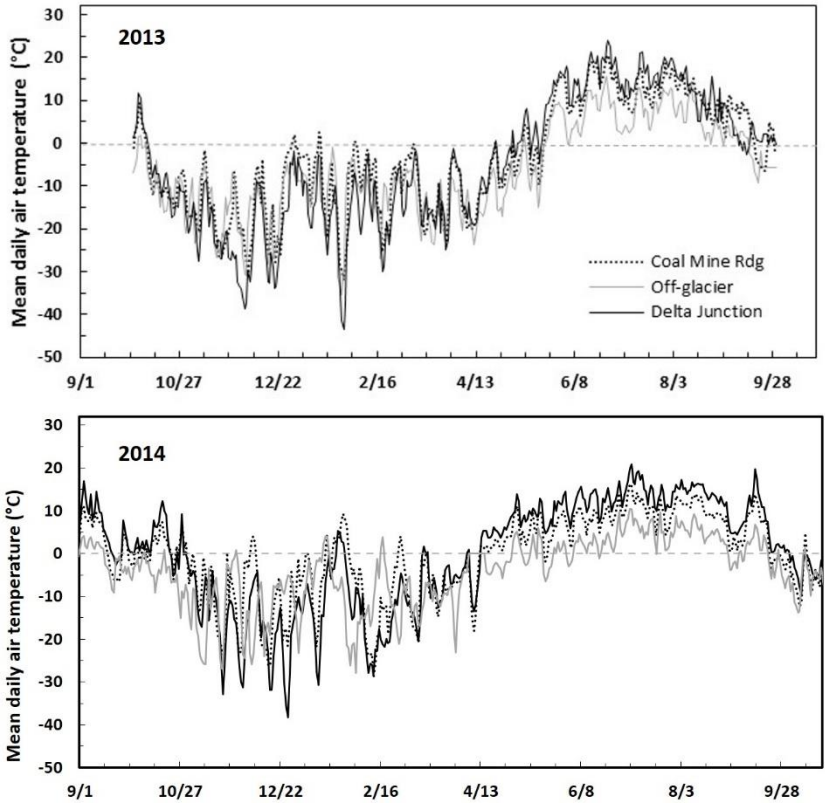

Figure 4. *Mean daily air temperature during the 2012-2013 and 2013-2014 hydrologic years at the low- (Delta Junction), mid- (Coal Mine Ridge) and high (Off-glacier) elevation sites.*

Distribution of mean summer (JJA) and winter (NDJ) air temperatures with elevation show opposite trends with season (Fig. 4). Winters present an inversion with high elevation sites recording relatively warm, average winter air temperatures compared to Delta Junction. A cooling trend in air temperatures with increasing elevation is found in summer with the largest rate of change between the two upper sites (840 and 1650 m). The lapse rates do differ somewhat between the twoyears.

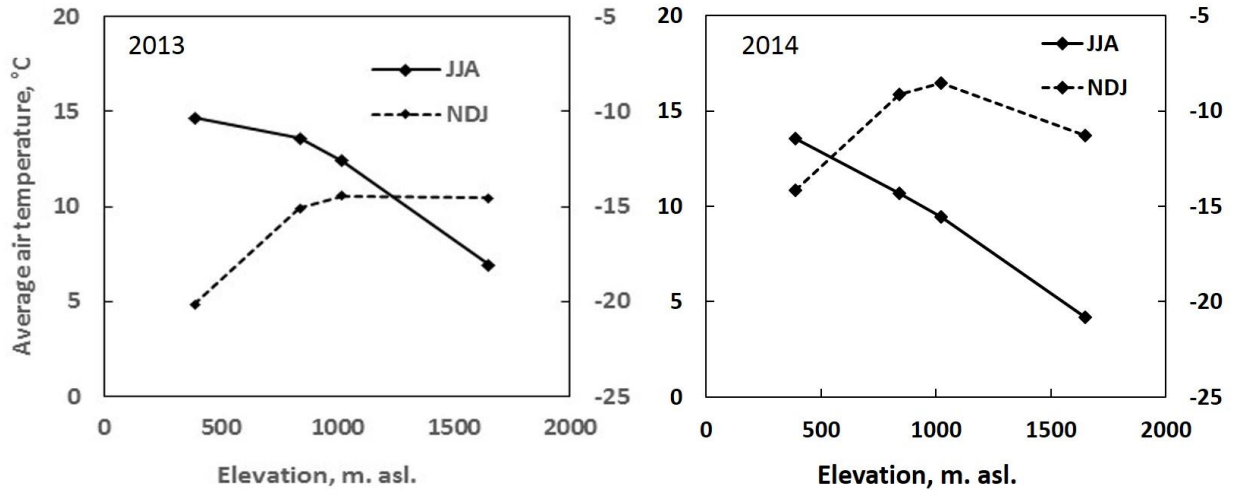

Figure 5. *Measured mean monthly winter (NDJ) and summer (JJA) air temperatures in 2013 and 2014 amongst four of the stations Delta Junction (389 masl), Coal Mine Road (840 masl), Coal Mine Ridge (1021 masl) and Off-Glacier (1650 masl) organized by elevation.*

Measured rainfall amounts in 2013 increase with elevation (Fig. 6). The total seasonal rainfall amount at McCumber (271 mm) was nearly twice that of Delta Junction (138 mm), while less differences were observed between individual mid-elevation stations (McCumber, Coal Mine Road and Coal Mine Ridge). In 2014, Delta Junction received similar amount of rainfall (242 mm) as the high elevation sites (238 to 225 mm). Summer 2014 had rainfall amounts in Interior Alaska. Interestingly, the high elevation rainfall was similar in 2013 and 2014. Therefore, one may conclude the summer 2014 extreme rainfall amounts were constrained to Interior Alaska and excluded the eastern Alaska Range. An individual rain event often occurred throughout all sites, but there were also several instances where rain was recorded at Delta Junction but not the high-elevation sites (>800 m) and vice versa.

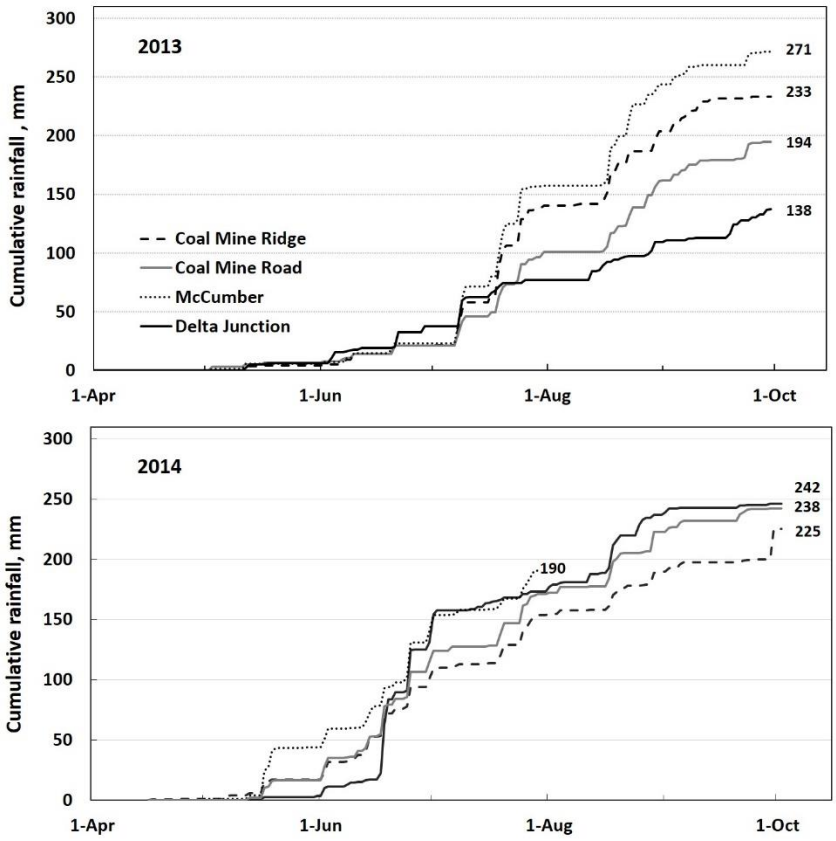

Figure 6. *Measured cumulative rainfall during the 2013 and 2014, Jarvis Cr. Seasonal totals are shown as individual numbers for respective site. The data is not corrected for under-catch.*

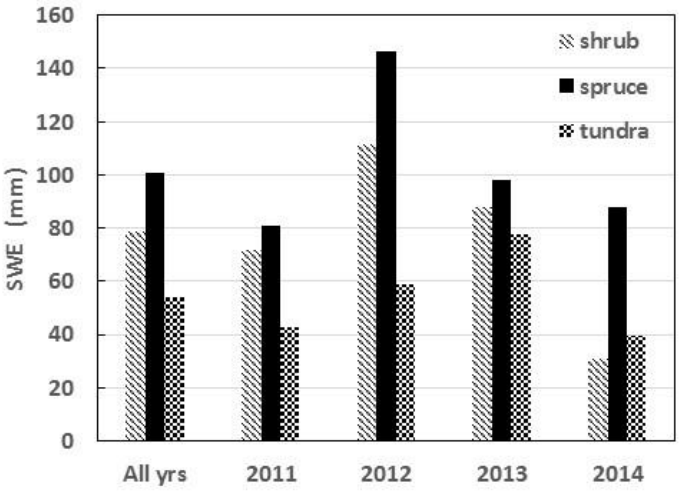

Figure 7. *Average end-of-winter snow accumulation presented as units of Snow Water Equivalent, SWE, of the three major vegetation types (alpine tundra, shrub and spruce forest). Measurements were made in late March-early April.*

3.1.2 Snow accumulation, Jarvis Cr.

End-of-winter snow surveys (late March-early April) via snow machine allowed for an estimation of the accumulated snow water equivalent prior the snowmelt. The snow surveys were according to the protocol described by *Rovansek et al.* (1996) where each survey included 50 depth measurements and five density samples.

End-of-winter snow accumulation in the tundra (alpine), shrub and forest (spruce) ecotypes was largest in the forest vegetation cover throughout year 2011-2014 (Fig. 6). In three of the four years, the second largest accumulation was measured in the shrub ecotype. The outlier of 2014 (alpine tundra SWE was larger than shrub) had a major snowmelt event in late January that resulted in runoff at the bridge. Overall, the SWE averaged 101 (spruce forest), 79 (shrub) and 54 mm (alpine tundra).

3.1.3 Glacier melt, Jarvis Cr.

Glacier melt was measured via ablation stakes, which were drilled into the glacier ice. The stakes were installed in spring (prior the onset of snowmelt) and included end-of-winter snow accumulation measurements on the glacier (snow depth and density). The glacier ice/snow surface in relation to the fixed stake was measured during visits in July and September. Stakes were re-installed as they melted out of the ice.

Total seasonal (Apr. – Sep.) melt of snow and ice increased as the elevation decreased (Fig 8). Total melt at the upper stake (1636 masl) ranged from 2.3 (2011) to 3.2 m (2013) of water equivalent, while the low elevation stake ranged from 4.2 (2012) to 5.5 m (2014). The melt was not continuously higher at the lower compared to the upper sites throughout the melt season. Early season melt (Apr.-Jul.) was larger at the lower two sites in all years, while late season melt (Jul.-Sep.) was lowest at the lower most glacier-centerline stake in 2012 and 2013. In 2014, the late summer melt was larger at the glacier-centerline at ~1550 m compared to the lowest stake. This phenomena can also be described as change in daily melt rate with elevation decrease/increase (mm day^{-1} m^{-1}). Late season melt rate between the upper and mid stakes was 0.12 mm day^{-1} m^{-1} in 2012, while the melt rate between the low and mid stakes was dramatically lower (0.03 mm day^{-1} m^{-1}). The low elevation stake was located in an area covered by debris, which suppressed the melt and also reduced the interannual variability in melt. Total annual mass balance present a near-linear correlation to elevation (Fig. x).

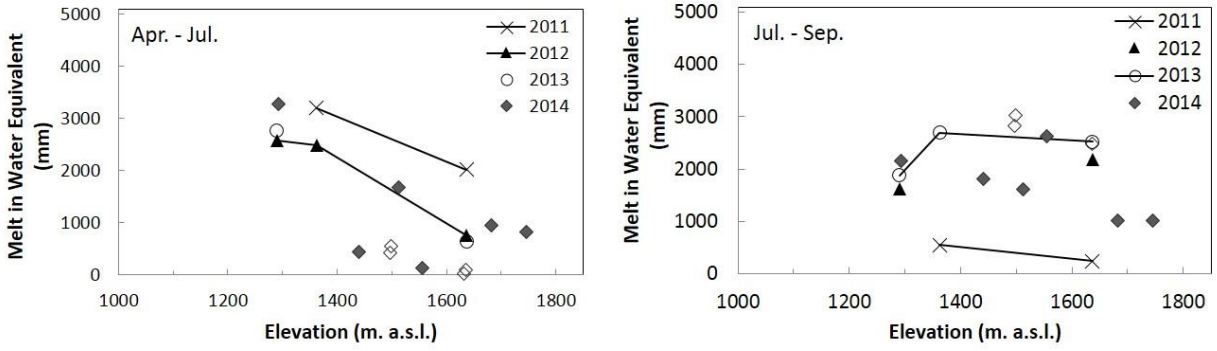

Figure 8. *Measured melt of snow and ice on the glacier during different time periods (Apr-Jul, Jul-Sep and Apr-Sep) in 2011, 2012 and 2013. The uppermost mass balance stake was located at 1636 masl. Solid rhombs (2014) represent stakes located along the glacier centerline, while open rhombs represent stakes located near the glacier sides.*

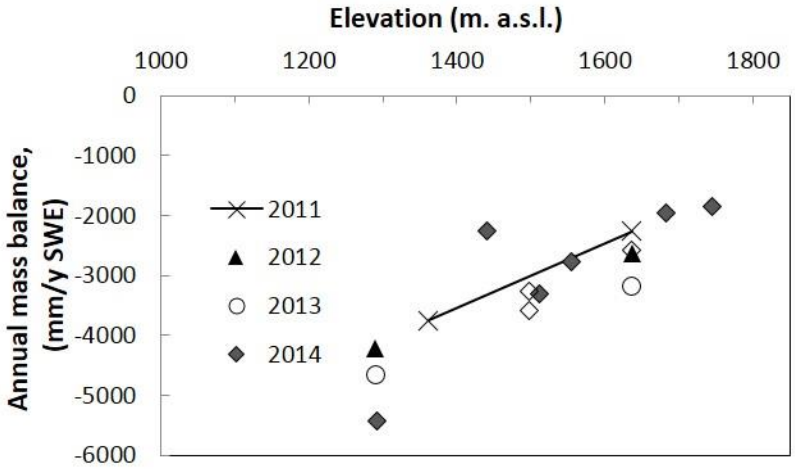

Figure 9. *Four years of measured annual glacier mass balance, Jarvis Cr.*

3.1.4 Stream water levels, Jarvis Cr.

Water levels were measured continuously where the Richardson Hwy Bridge crosses Jarvis Cr. Diurnal fluctuations were observed throughout the season, with the highest water levels corresponded to rain storms in late summer. The early season (mid/late May) stream water levels (snowmelt) were similar to peak magnitudes in late summer/early fall in 2013. Lowland snowmelt was rather late in 2013 (mid- to late-May). In 2014, no pronounced snowmelt peak in April/early was observed due to the earlier melt even in late January.

3.1.5 Runoff, Jarvis Cr.

Runoff at Jarvis Cr. was measured just upstream of Jarvis Cr. confluence with the Delta River (Richardson Hwy Bridge) in summer and further upstream in winter ("Niki site"). A handheld electromagnetic flowmeter (Marsh-McBirney) was used when the waters were safe to cross by foot, which was typically only during late-May/early-June and prior freeze-up (mid-Sep and onwards) in Jarvis Cr. At other time, the discharge was measured with an Acoustic Doppler Current Profiler, ADCP, (StreamPro, Teledyne) mounted to a smaller boat, which was ferried across the channel using a pulley-rope system spanning the entire river cross section.

The time lag between a rainfall event (Coal Mine Ridge) to peak runoff (Bridge) was calculated from four larger rain events (ranging from 7 to 25 mm) in July 2013. Lag-times, defined as the time between the centroid of the rain event to the peak runoff, averaged about 10 h (9 to 13.5 h).

Table 4. *Discharge measured with FloMate (*) and A DCP in 2013 and 2014 at the Richardson Hwy Bridge, Jarvis Cr. Italicized observations in parentheses are questionable due to poor estimation of channel depth with no sonic depth sounder mounted to the StreamPro. A separate sonic sounder was added prior the 2014 season.*

Date	Discharge (cms)
6/12/13	7.2*
7/2/13	12.2
7/3/13	11.9
7/3/13	12.6
(7/10/13	*17.8)*
7/11/13	12.4
7/11/13	10.6
7/17/13	13.6
8/8/13	13.1
8/15/13	12.8
(8/19/13	*16.1)*
(8/19/13	*16.6)*
(8/19/13	*16.6)*
(8/20/13	*14.3)*
(8/21/13	*15.1)*
8/21/13	13.8
10/1/13	3.1
10/3/13	3.5*
10/10/13	2.4*

Date	Discharge (cms)
5/14/2014	2.4*
5/19/2014	4.6*
5/24/2014	3.6*
6/12/2014	5.3*
6/12/2014	5.3*
6/12/2014	4.9*
6/12/2014	4.8*
6/12/2014	4.5*
6/25/2014	28.9
6/25/2014	28.9
6/26/2014	19.1
6/26/2014	22.7
6/26/2014	19.5
6/26/2014	19.1
6/26/2014	22.7
6/26/2014	19.5
6/27/2014	14.5
6/27/2014	13
6/27/2014	14.5
6/27/2014	13

Date	Discharge (cms)
7/1/2014	20.7
7/1/2014	21.6
7/1/2014	20.7
7/1/2014	21.6
7/2/2014	21.1
7/2/2014	21.1
7/3/2014	11.2
7/3/2014	11.2
7/10/2014	11.5
7/16/2014	11
7/24/2014	10.8
7/28/2014	10.4
7/28/2014	10.05
7/28/2014	10.2
7/30/2014	12.5
7/30/2014	10.7
7/31/2014	12.4
8/19/2014	12.7
9/3/2014	7.1
9/20/2014	10
9/28/2014	3.3*
10/1/2014	2.8*

Winter runoff measurements (located between N63° 47.669' and N63° 45.859') decreased from 2.2, 2.1 to 1.5 cms as the season progressed (18 Nov., 22 Jan., 6 Mar., respectively), although an atypical melt event in late January (~Jan. 27th) resulted observations of significant flows downstream at the bridge.

A stage-discharge curve was established using measured runoff and hourly water levels (Fig. 10). Evaluations of the StreamPro measurements in 2014 concluded that the measurements were not reliable at discharges >14 cms without a separate sonic depth sounder due to the large sediment load in the water column. A sonic sounder was added to the system prior the 2014 season. Estimated runoff present diurnal variations throughout late May until late Sep. in 2013 (Fig. 11). Baseflow appears at its highest in late July/early August in both years. Peak flows in 2013, which were estimated to approache 20-25 cms, were concentrated to the late snowmelt in May/early and again during individual larger rain events in mid- to late summer, with the last high flows in early Sep. The peakflow in 2014 was measured with the ADCP on June 28th (29 cms) and coincided with an intense rain event. The peakflows in 2014 were constrained to the early summer, despite some rather significant rain events recorded in Delta Junction. The cooling of air temperatures at the glacier, but also in the lowlands (Fig. 4), and the lack of rainfall in mid-/late Sep. resulted in a dramatic decline in flow from ~10 cms to < 5 cms within a 2-week time period in 2013. In 2014,

a warm spell in September supported a smaller peak. Overall, the estimated specific summer runoff totaled 200 mm (May 22 - Oct. 3rd).

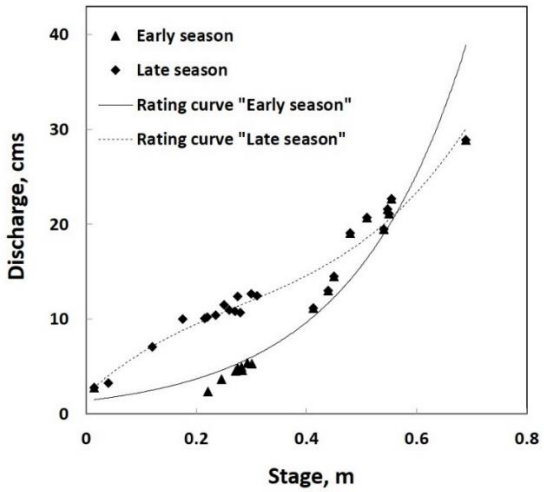

Figure 10. *Established stage-discharge relationships used for estimating the continuous 2013 and 2014 hydrographs. The 2014 stage-discharge relationship was applied to the 2013 stage via a linear shift of the 2013 stage (a linear regression between 2013 and 2014 stages that produced similar magnitude discharge measurements) The mean error of the 2013 stage-discharge relationship is estimated to ±0.2 cms.*

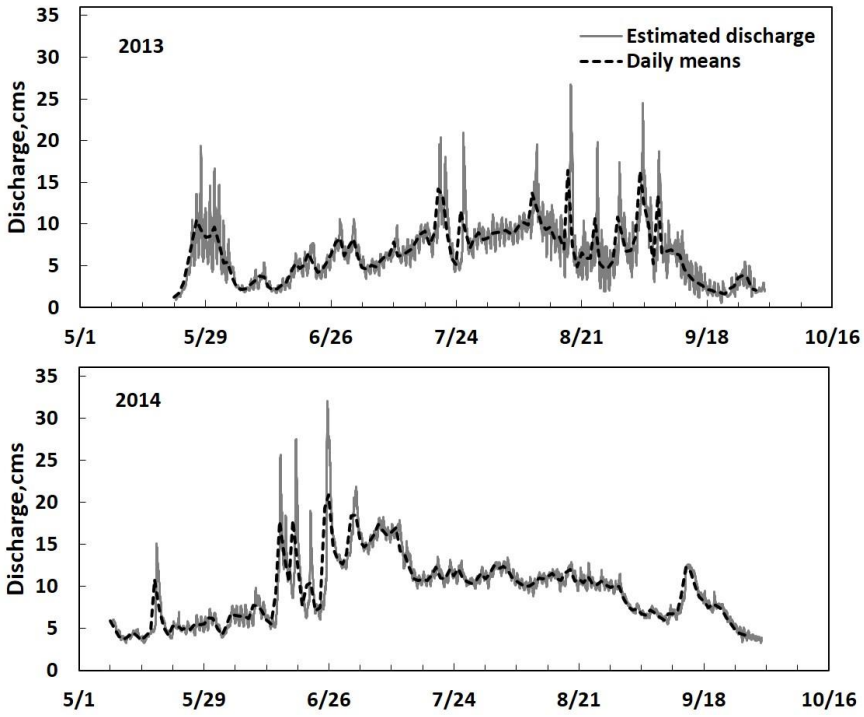

Figure 11. *Estimated continuous (hourly and daily) runoff, Jarvis Cr., near the Richardson Hwy in 2013 and 2014.*

3.1.6 Climate projections, Jarvis Cr.

High-resolution dynamic downscaling simulations and projections were conducted in order to fully make the coarse-resolution GCM results useful for accurate assessments of climate change impacts at the regional scales. Built-upon our previous and on-going research efforts and accomplishments, we employed the Weather Research and Forecasting (WRF) model configured at a horizontal resolution of 20 km for the downscaling simulations. To achieve the best performance, we optimized the WRF model configurations for our application, including setup of vertical levels, selection of model physical treatments, and nudging techniques for large-scale forcing by using existing reanalysis products and the GCM outputs. CCSM4 21st Century Projections under the RCP6 mitigation scenario from the same MOAR ensemble member provides the initial & boundary conditions for the WRF model. The results were used to inform the DETIM glacier model and the WaSiM hydrology-glacier model.

Throughout the 20 km resolution study domain, the following major changes were projected under the RCP6.0 scenario:

- significant warming trend in both daily maximum and minimum temperatures
- strong summer daily maximum warming in the southeastern part of domain (probably due to reduced snow cover), while strong winter daily minimum warming in the northwest.
- reduced snow cover (SWE) by ~50% by the end of century
- enhanced precipitation particularly in summer.

Three grid points, representing the location and elevation of Delta Junction, Coal Mine Ridge and Off-glacier sites, were used to force WaSiM. Here the average projected increase in mean annual temperature was estimated to 0.6 ºC per decade during the earlier time period (1990-2030) throughout all three sites and about a magnitude less (0.02-0.04 ºC per decade) during the later period (2030-2075) with the larger rates at higher elevation (Table 5, Figure 12). The average change in mean annual air temperature amongst all the sites would be a 2 ºC warming (1990-2010 to 2055-2075). Mean annual precipitation on the other hand would see about a 9% decrease (758 to 690 mm) (Table 6).

Table 5. *Projected average increase in mean annual air temperature at the three locations from 1990 to 2030 and from 2030 to 2075.*

	1990-2030 (ºC yr^{-1})	2030-2075 (ºC yr^{-1})
Delta Junction	0.059	0.0016
Coal Mine Ridge	0.058	0.0028
Off-glacier	0.055	0.0037

Table 6. *Projected average mean annual air temperature (MAAT) and precipitation (MAP) during the four periods representing all three locations (Delta Junction, Coal Mine Ridge and Off-glacier).*

	MAAT (ºC)	MAP (mm)
1990-2010	-6.4	758
2015-2034	-5.1	712
2035-2054	-4.6	753
2055-2075	-4.4	690

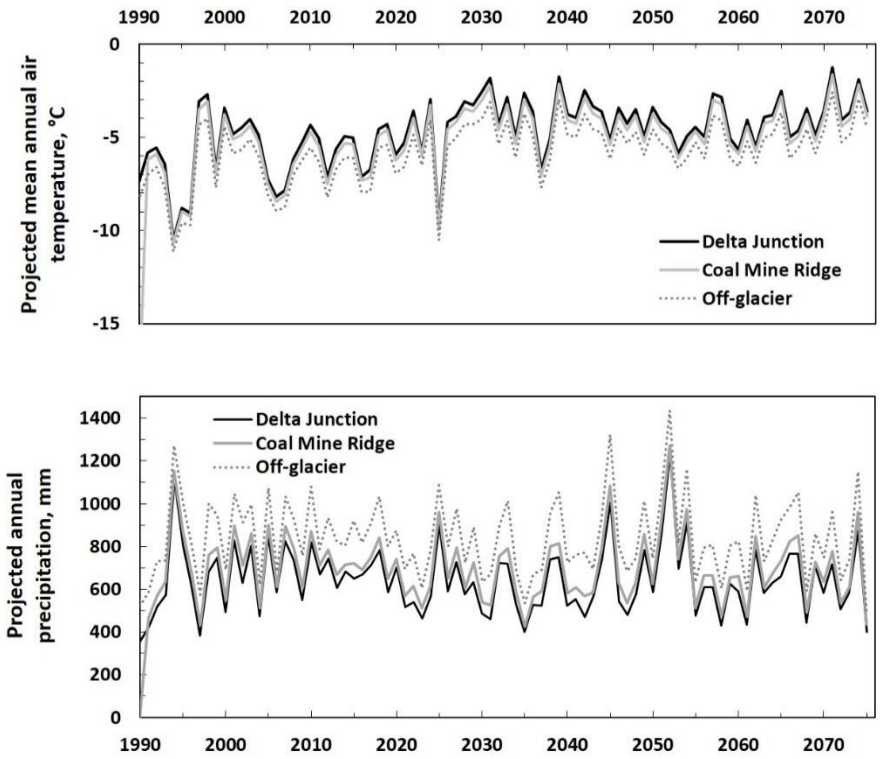

Figure 12. *Projected mean annual air temperature and total annual precipitation at the three locations. Results from downscaled climate simulations performed at 20 km spatial resolution.*

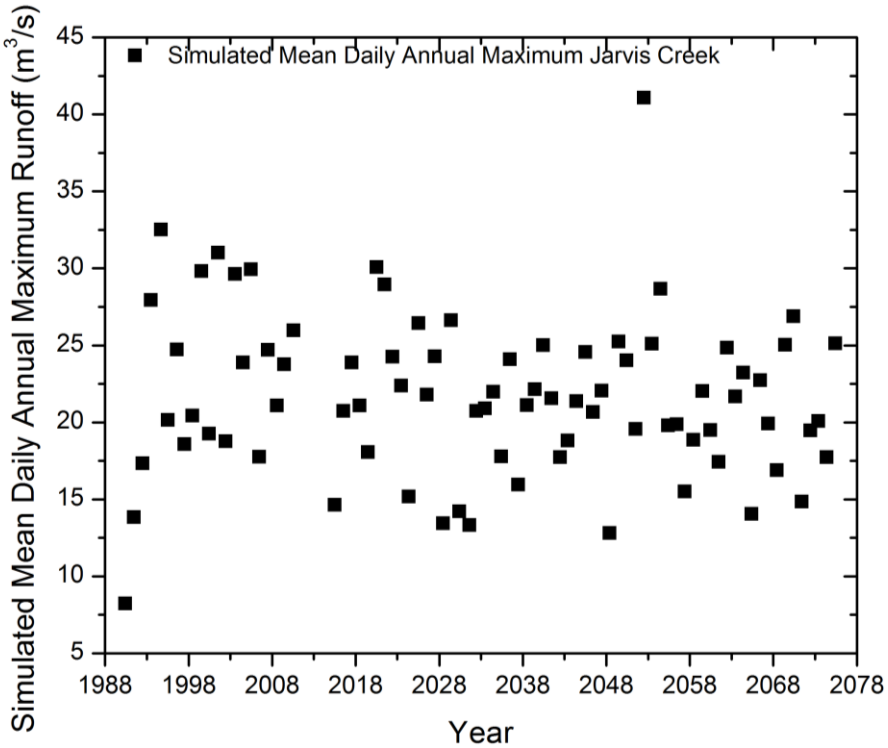

Figure 13. *Simulated mean daily annual maximum runoff, 1990-2010 and 2015-2077, Jarvis Cr.*

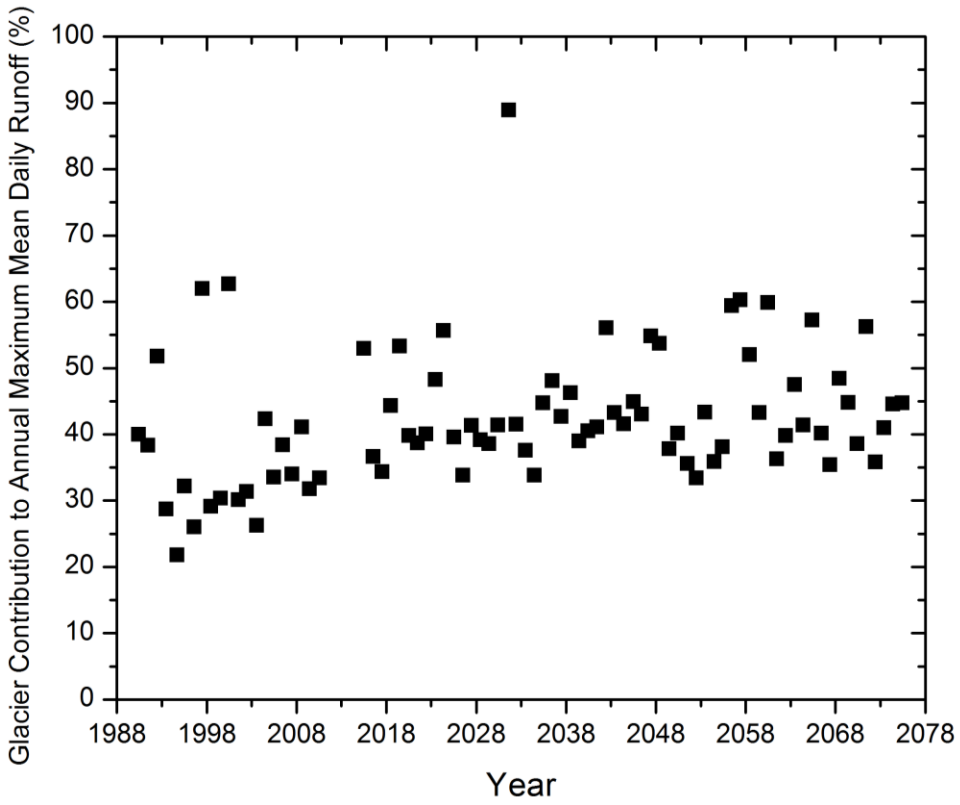

Figure 14. *Simulated glacier contribution to annual maximum mean daily runoff, Jarvis Cr.*

3.1.7 Flow frequency analysis, Jarvis Cr.

A flow frequency analysis was conducted to examine the frequency of events on Jarvis Creek at Richardson Highway. Analyses were completed according to the Interagency Advisory Committee on Water Data, Hydrology Subcommittee, Bulletin 17B (Log Pearson III distribution) using HEC software. The analysis was performed using annual maximum daily flow data from model simulations. The hydrological model WaSiM (Schulla, 2013) was used at a daily time step to produce long-term projections of runoff and glacier contributions.

The flood frequency analysis would be improved if we looked at instantaneous peak flows, i.e not mean daily values. Additionally, we recognize that the annual maximum flow event may be generated by snowmelt, rainfall, or glacial melt, or a combination of these processes, thus the peak event for any given year may not be independent and homogenous. The standard frequency approach was used for the mixed population, only one annual maximum flow event was examined regardless of whether it was generated by rainfall, snowmelt, or glacier melt. The analysis could be improved if we looked at events generated by different hydrologic processes individually. A weighted skew was calculated based on the regional generalized skew for Alaska Region 6.

Table 7. *Simulated mean daily peak flows. Note, a large flood was simulated during the 2036-2055 period, which caused the skewness to change signs.*

Analysis	Period of Record	Number of annual events	Number of low outliers	Number of high outliers	Weighted Skew	Station Skew
1	1990-2010	21	1	0	-0.188	-0.298
2	2015-2035	21	0	0	-0.259	-0.397
3	2036-2055	20	0	1	0.258	0.304
4	2056-2075	20	0	0	-0.159	-0.261
5	1990-2010, 2015-2076	82	1	0	-0.032	-0.046

The analysis is divided into four periods of approximately 20 year increments, the first period is from 1990-2010, second period is 2015-2035, third period is 2036-2055, and the fourth period is from 2055-2075. Table 1 presents the skewness for each analysis period. A positive skewness indicates the mean peak flow exceeds the median peak flow. A negative skewness indicates the median peak flow exceeds the mean peak flow. All analyses had negative skew coefficient with the exception of period three, 2036-2055, due to an extreme event causing the skew to be positive

For the analysis period of 1990-2010, the percentage of runoff during the annual flood that may be attributed to glacial melt ranges from 22 to 63% (Fig. 14). Four years (1990, 1992, 1997, and 2000) have a glacier contribution to peak runoff of greater than 50%. Only one year (1994) has a glacier contribution of less than 25% and this year was the highest maximum flow event (rank = 1) during the analysis period (with a return period of 22 years). For the analysis period of 2015-2035, the percentage of runoff during the annual flood that is attributed to glacial melt ranges from 34-89%. Four years (2015, 2019, 2024, and 2031) have a glacier contribution to peak runoff of greater than 50%. In the analysis period 2036-2055, the percentage of runoff during the annual flood attributed to glacial melt ranges from 33-56%. Three years have a glacier contribution to peak runoff greater than 50%. In the analysis period 2056-2075, the percentage of runoff during the annual flood that can be attributed to glacial melt ranges from 35-60%. Six years have a glacier contribution to peak runoff greater than 50%. Overall, the lower, but more frequent, floods have a higher relative glacial input. This large contribution of glacier melt during the lower peak flows are likely causing the data to "jog" somewhat in the exceedance probability plot for the entire simulation period (Fig. 15).

A slight overall decrease in the annual mean daily maximum runoff is observed through the entire simulation 1990 to 2075 (Fig. 13). Although the glacier contribution to the simulated annual maximum runoff appears to increase over time, especially during the first few decades (1990-2030), the highest flood events tend to have less glacier contribution, indicating that rainfall or snowmelt generated events may have a greater influence (than glacier melt) during the highest flood events. However, we did not perform a partial duration flood analysis to assess whether floods events are increasing in number. Expanding the analysis beyond just assessing one flood per season to include multiple floods per year (for example, all floods above a certain discharge) would allow us to quantify whether there are more frequent floods occurring above a certain threshold.

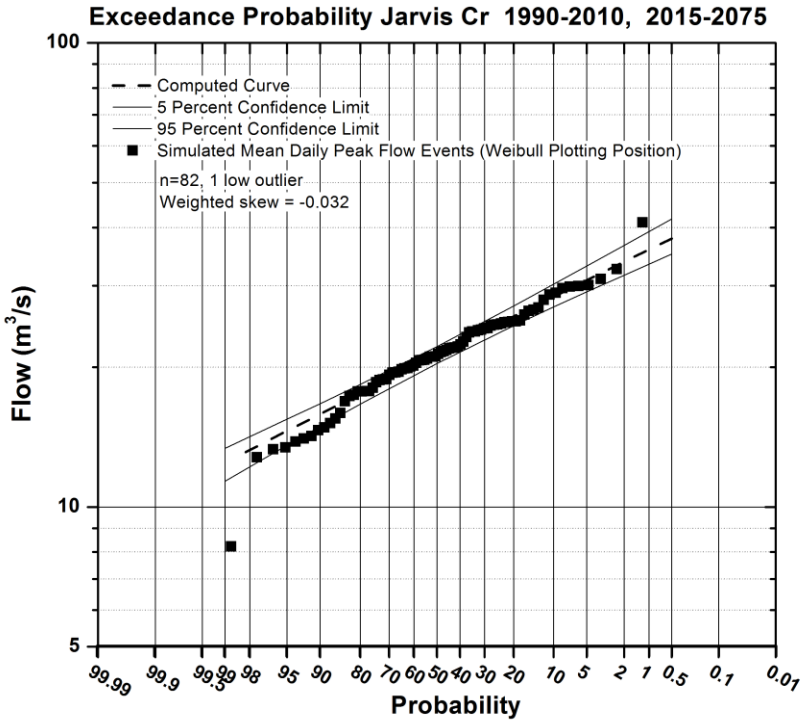

Figure 15. *Exceedance probability plot for entire simulation (1990-2010 and 2015-2075, Jarvis Cr. Flows are simulated mean daily annual maximum.*

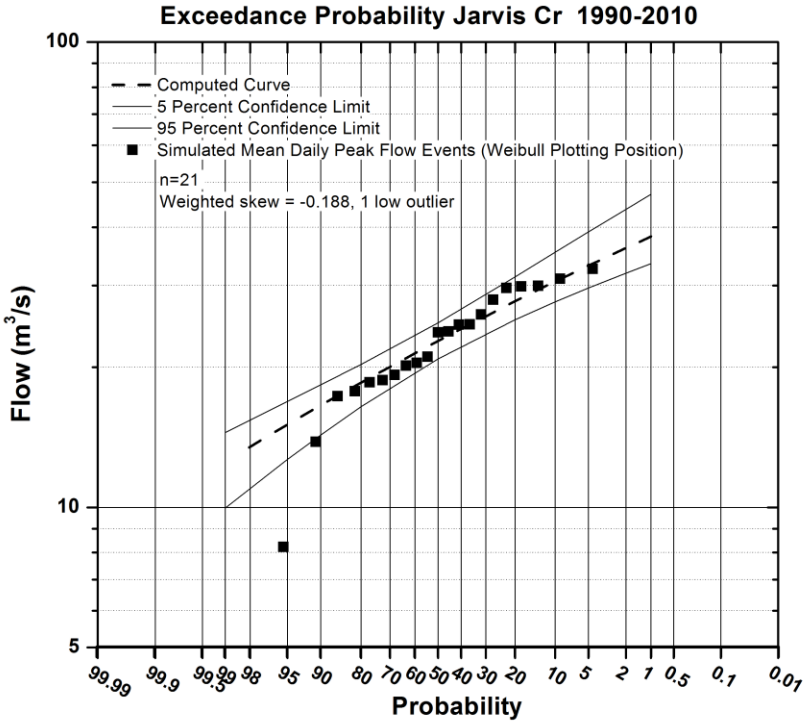

Figure 16. *Exceedance probability plot for simulation period 1990-2010, Jarvis Cr. Flows are simulated mean daily annual maximum.*

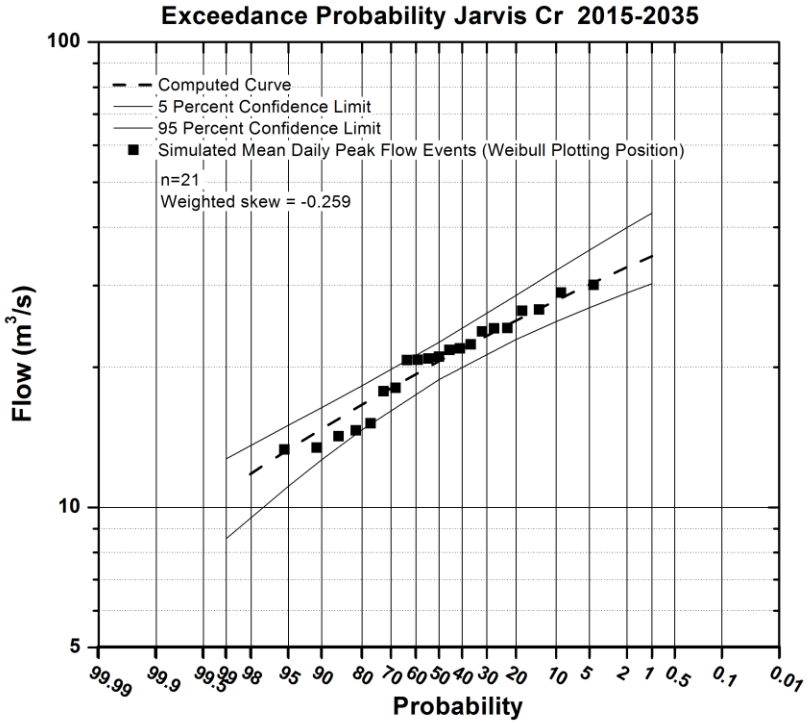

Figure 17. *Exceedance probability plot for simulation period 2015-2035, Jarvis Cr. Flows are simulated mean daily annual maximum.*

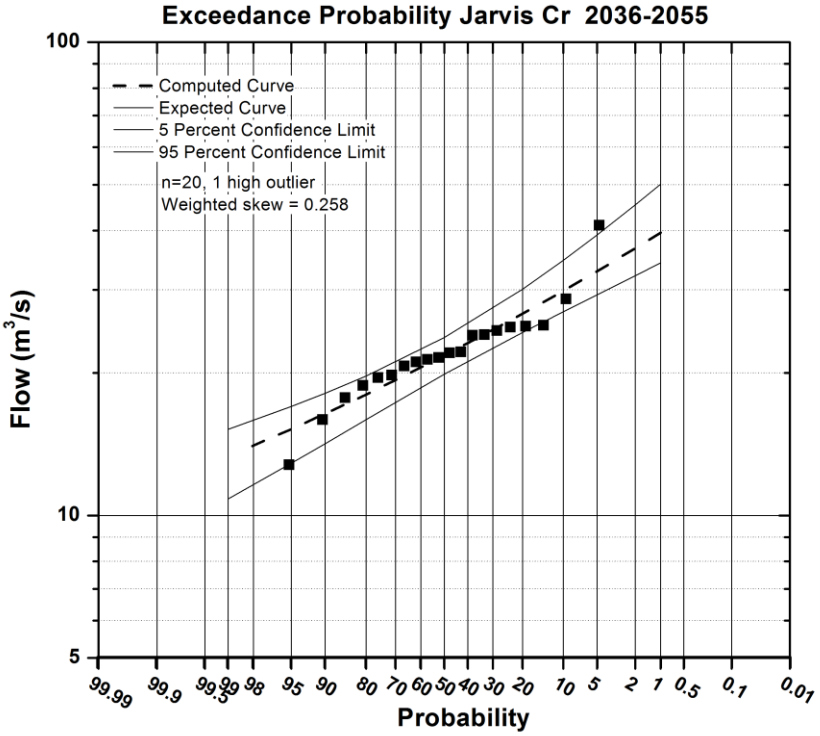

Figure 18. *Exceedance probability plot for simulation period 2036-2055, Jarvis Cr. Flows are simulated mean daily annual maximum.*

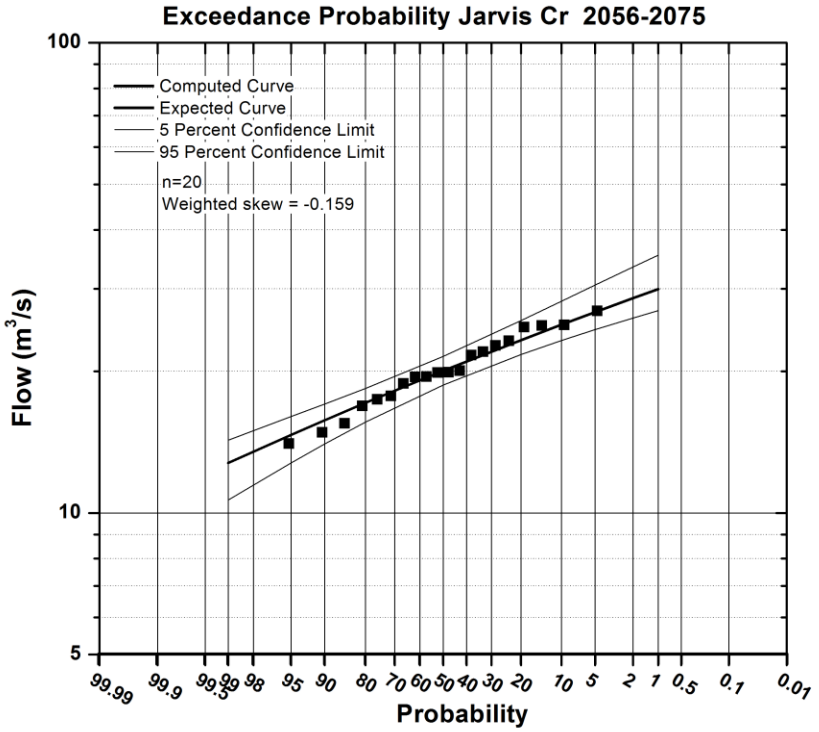

Figure 19. *Exceedance probability plot for simulation period 2056-2075, Jarvis Cr. Flows are simulated mean daily annual maximum.*

3.2 Valdez Glacier Stream

3.2.1 Meteorology, Valdez Glacier Stream

Three HOBO Pro v2 U23-001 air temperature and relative humidity (T/RH) sensors were installed on the glacier on April 19, 2012, using a floating temperature stand to maintain the height of the sensor (2 m) above the glacier surface throughout the melt season (Fig. 2, Table 8). Two off-glacier weather stations were constructed on ridge tops adjacent to the glacier, at elevations of 486 m (labelled "Prospector") and 1465 m (labelled "Schrader"). The Prospector station was located in shrub tundra on the southern flank of the east branch of the glacier, and the Schrader station was on exposed bedrock on a ridge above the accumulation area. Each off-glacier weather station was equipped with a Campbell Scientific 107-L temperature sensor, a 41303-5A 6-gill radiation shield, and a Campbell Scientific TE525WS-L tipping bucket rain gauge. Equipment failures and wildlife disturbance resulted in several data gaps at the two off-glacier weather stations.

A comparison of air temperature on- and off the Valdez glacier shows that the Prospector station (486 m asl) experienced higher mean daily air temperatures than the lowest on-ice temperature sensor (380 m asl) (Fig. 20). This shows that temperatures are lower on the glacier compared to temperatures recorded outside the glacier surface at similar elevations. Accordingly, bias-correction of off-glacier air temperature records are important for melt modelling. The mean daily air temperatures observed at the Schrader station (1465 m asl) were comparable to those temperatures observed at the upper on-glacier sensor (1495 m asl), and even indicate lower mean daily temperatures than those observed at the upper on-glacier sensor. Average annual air

temperature at the Valdez VSO (Town of Valdez) was 3.3 ºC in 2012-2013 hydrologic year with minimum and maximum mean monthly values ranging from −5.9 ºC to 14.9 ºC (Table 9).

Rainfall data collected at each ridge top weather station is plotted in Fig. 21, along with rainfall from the NOAA WSO. The WSO recorded precipitation amounts that were greater than those recorded at the Prospector and Schrader sites. This was likely due to undercatch by the unshielded tipping bucket gages used at the Prospector and Schrader sites, and the fact that both stations were on high elevation ridges that likely experienced high winds, reducing precipitation catch. The measured precipitation was compared to the mean monthly normal from the PRISM dataset representing 1705 masl, suggesting more than twice the amount of summer season precipitation at 1705 masl compared to 11 masl (Valdez VSO). The PRISM dataset of Valdez VSO location show relatively good agreement to measurements (Figure 22, 23).

Table 8. *Location of meteorological and hydrological stations, Valdez Glacier Stream watershed.*

Site name	***Variable***	***Vegetation***	***X***	***Y***	***Elev. (masl)***
Transducer A	Lake water level	Deciduous	544572	6780041	68
Transducer B	Air pressure	Deciduous	544445	6779630	71
ADCP Transects	Runoff	Deciduous	544825	6779466	70
Valdez WSO	Meteorology	Deciduous	534823	6777612	11
Lower Glacier	Meteorology	Glacier	545163	6788323	381
Middle Glacier	Meteorology	Glacier	542816	6795136	821
Upper Glacier	Meteorology	Glacier	533753	6802648	1326
Prospector	Meteorology	Shrub	546030	6786717	486
Schrader	Meteorology	Bedrock	545715	6796714	1465

Table 9. *Mean monthly air temperatures (ºC), Valdez Glacier Stream watershed.*

	2012			**2013**									
	Oct	**Nov**	**Dec**	**Jan**	**Feb**	**Mar**	**Apr**	**May**	**Jun**	**Jul**	**Aug**	**Sep**	*Mean*
Valdez Town	2.8	-3.8	-5.9	-3.2	-1.4	-2.1	-0.3	5.9	14.0	14.9	12.9	9.8	*3.1*

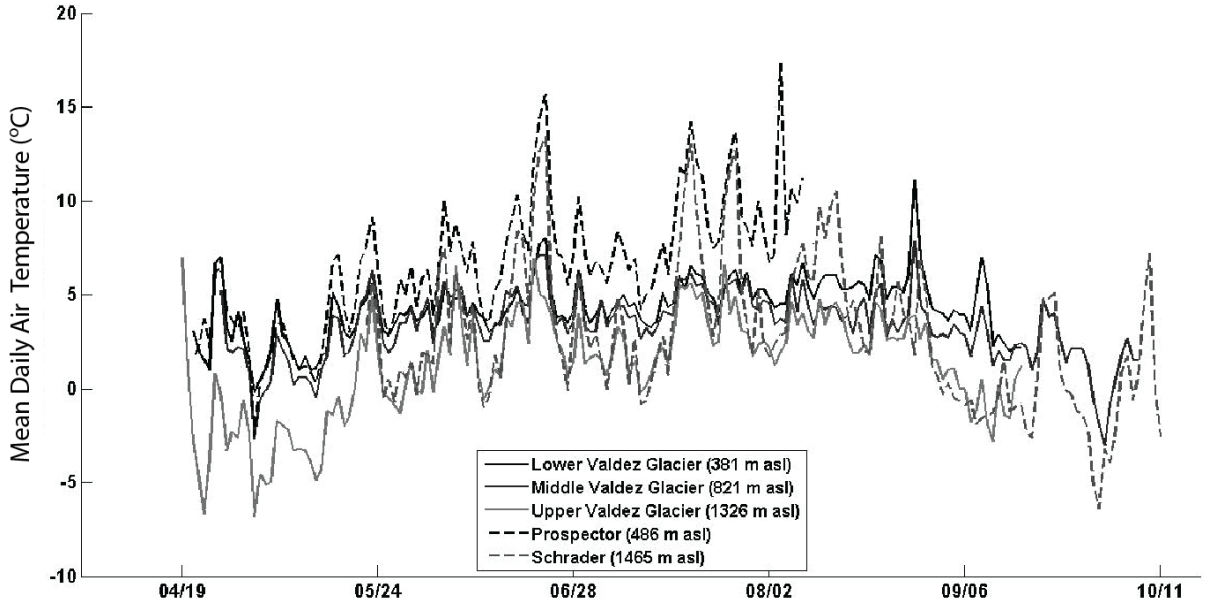

Figure 20. *Mean daily air temperature at three station on the Valdez Glacier (lower, middle and upper) and two ridge top stations (Prospector and Schrader) during the summer of 2012.*

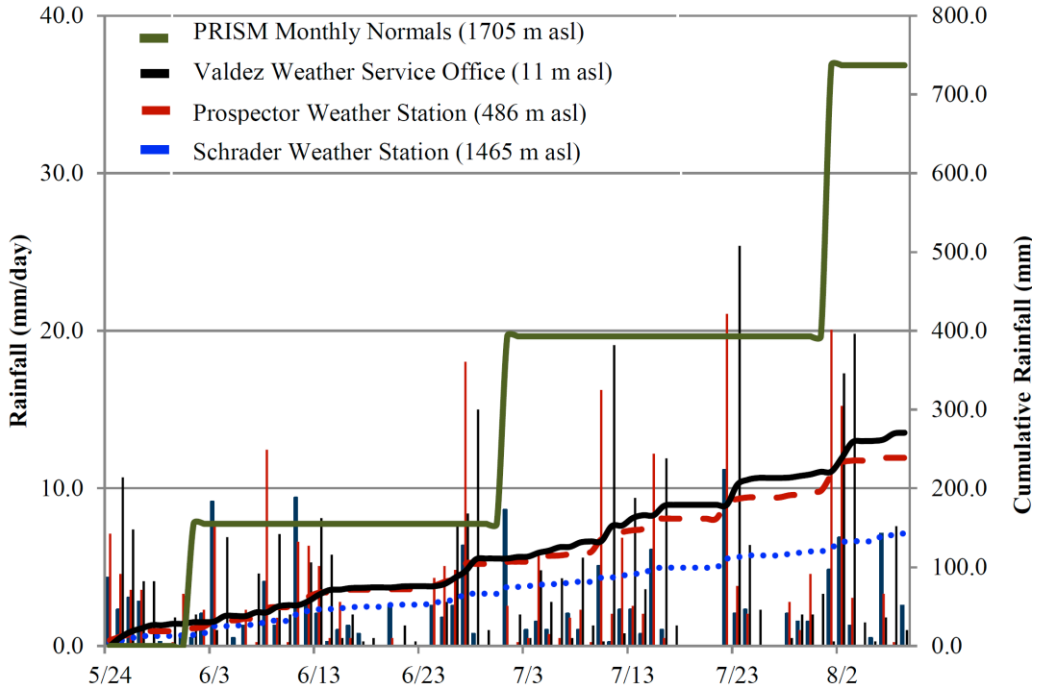

Figure 21. *Measured cumulative rainfall during summer 2012 two ridge-top stations (Prospector and Schrader) near Valdez Glacier and the NWS station at the town of Valdez.*

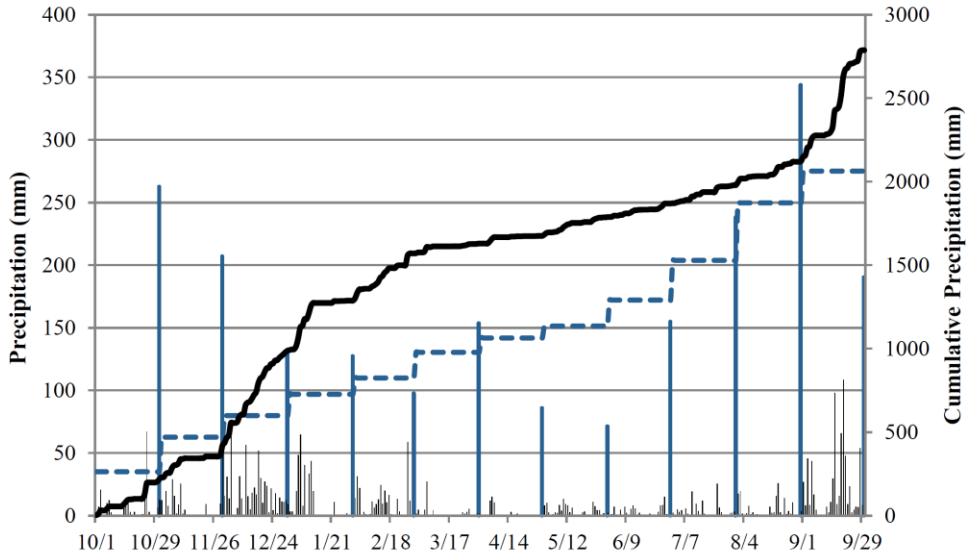

Figure 22. *Precipitation from Valdez VSO (black) at 11 masl and PRISM monthly normals at 1705 masl (blue) for hydrologic year 2011-2012.*

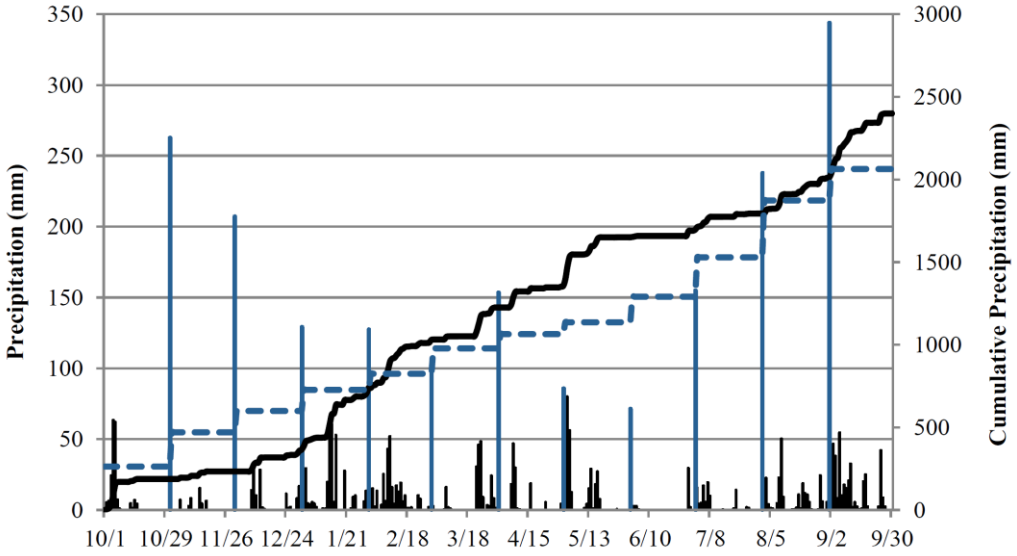

Figure 23. *Precipitation from Valdez VSO (black) at 11 masl and PRISM monthly normals at 1705 masl (blue) for hydrologic year 2011-2012.*

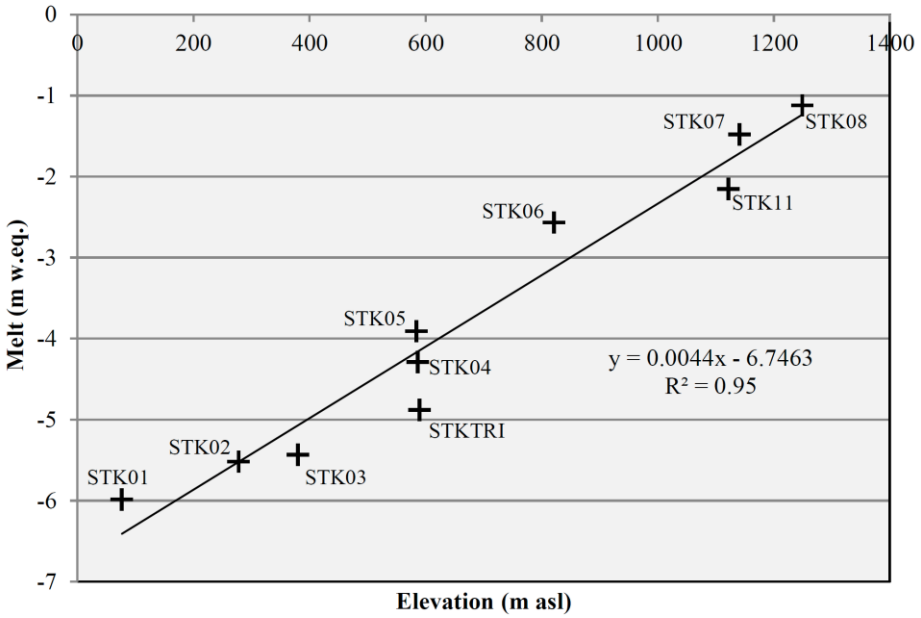

Figure 24. *Total glacier (ice, firn and snow) melt from mid-Apri through midl-Oct 2012 as measured with 10 ablation stakes.*

3.2.2 Lake water levels, Valdez Glacier Stream

Lake water level (Fig. 25) was measured using a HOBO U20-001-01 sensor installed in a steel pipe the along the northwestern shore of Valdez Glacier Lake (Transducer A, Fig. 3). A second transducer of the same type was deployed in the air to correct for barometric air pressure (Transducer B). Both sensors sampled at 15-minute intervals.

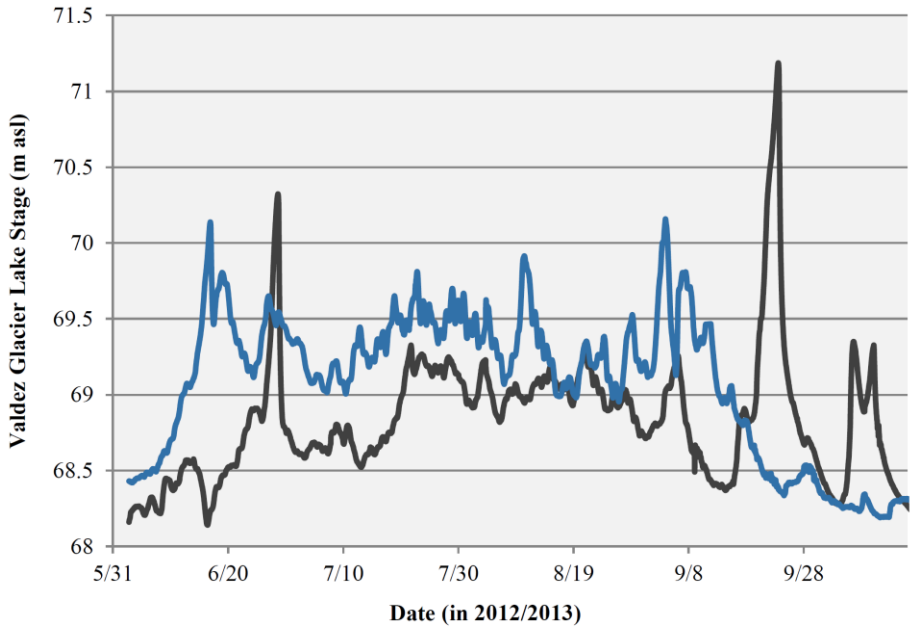

Figure 25. *Water level variations at Valdez Glacier Lake in 2012 and 2013.*

3.2.3 Measured Runoff, Valdez Glacier Stream

Runoff from the Valdez Glacier watershed was determined by calculating the relationship between lake water level and discharge. Lake (rather than river) stage observations were carried out due to difficulties encountered in measuring flow at a downstream location during the 2012 field season, and due to erosion of the river bed at the 2012 measurement site. Our method follows similar lake stage observations employed to assess glacial watersheds within which runoff is intercepted by a proglacial lake (e.g. Neal and Host, 1999). An analysis of the energetics of the Valdez Lake outlet stream relative to its bed composition suggests that the bed is suitably stable for establishing a rating curve at this location.

Table 10*. Discharge measured with the ADCP at Valdez Glacier Stream in 2012 and 2013.*

Transect ID Number	Date, Time	Gage Height (m asl)	Discharge ($m^3 s^{-1}$)
--	5/31/2012, 1130	68.279†	14.8 ± 2.47
--	5/31/2012, 1530	68.230†	16.4 ± 2.47
--	5/31/2012, 1940	68.322†	19.2 ± 2.47
--	6/1/2012, 1000	68.308†	11.1 ± 2.47
--	7/13/2012, 2245	68.783†	35.3 ± 2.47
--	7/14/2012, 1000	68.792†	34.5 ± 2.47
--	7/14/2012, 1400	68.811†	45.6 ± 2.47
--	7/14/2012, 1800	68.833†	50.7 ± 2.47
--	7/15/2012, 1800	68.844†	52.5 ± 2.47
1*	9/15/2012, 1330	68.359	22.5 ± 1.4
1	9/11/2013, 1315	69.406	156.5 ± 2.9
2	9/12/2013, 1045	69.391	148.9 ± 7.4
3	9/13/2013, 1022	69.004	92.8 ± 0.6
4	9/14/2013, 1126	68.863	74.8 ± 1.8
5	9/15/2013, 1655	68.960	85.4 ± 2.6
6	10/23/2013, 1130	68.191	13.2 ± 0.6

†Note: Listed gage heights were calculated using the 2013 rating curve. The transducer was relocated on September 13, 2012. Measurements conducted prior to September 13, 2012 were not used for modeling exercises. Error for these measurements was calculated using the average standard deviation observed in the 2013 measurements.

Total discharge was measured using either a StreamPro Acoustic Doppler Current Profiler (ADCP) or a River Ray ADCP. Discharge was measured on a periodic basis to capture the flow during a range of lake stages indicated by the pressure transducer in Valdez Glacier Lake (Table 7). A rating curve was established based on a linear fit of discharge to lake stage (Fig. 12). Continuous runoff was estimated by solving for discharge as a function of lake stage (Fig. 13), based on the 2013 rating curve.

The total estimated specific runoff was 3914 mm over the 2013 measurement period (May 26 – Oct. 24). Large fluctuations in flow occurred in relative short time period (up to 82 cms occurring within a 24 hour time span, June to mid-Sept.) .there were several. These diurnal flow variation reduced in late Sept. and Oct., with the exception of heavy rainfall events that occurred near the end of the measurement period.

Five large peak flow events occurred in 2013 (June 16, July 22, Aug. 11, Sept. 4, and Sept. 7) (Fig. 13). Air temperatures throughout the measurement period remained above freezing, indicating a steady generation of glacial melt. Based on climate data, it appears that the June 16 event is most likely a result of rapid increases in air temperature (e.g. snowmelt) resulting in a peak daily discharge of 214.5 cms. The runoff peak on July 22 coincides with a spike in air temperature, as well as a rainfall event that occurred on July 20. The Aug. 11 peak flow event was preceded by a rainfall event that spanned from Aug. 9 – 11, with the maximum rainfall of 50 mm (Valdes weather station) occurring on Aug. 10. The two peak flow events in early September occurred in the midst of a longer period of rain (Aug. 31 - Sept. 18), of which the two largest rainfalls occurred immediately prior the high-flow events. The Sept. 4 peak flow event is the largest observed in the hydrograph, and is estimated to 228 cms (note that the largest measured runoff was 156.5 cms).

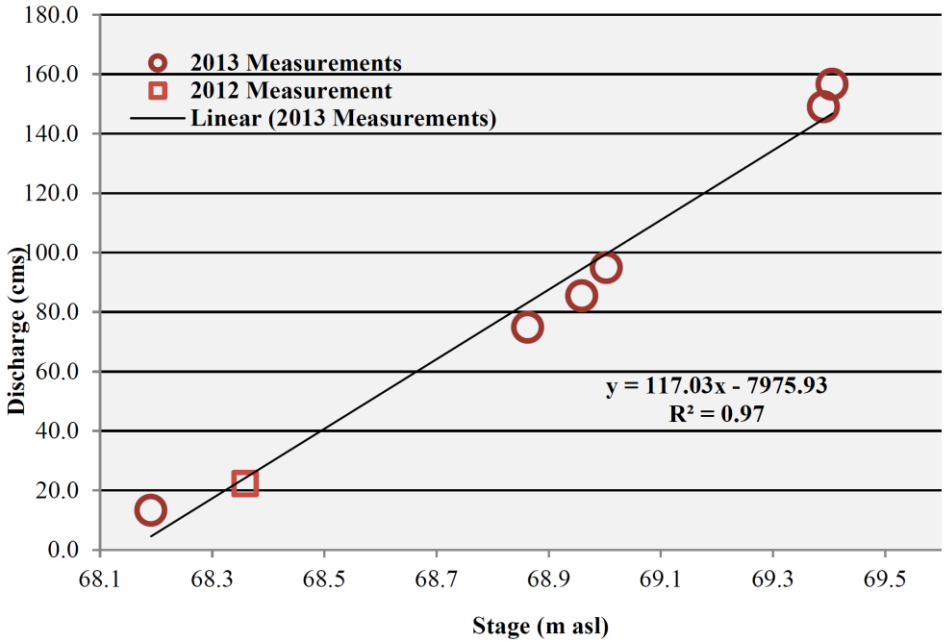

Figure 26*. Stage-discharge relationship at Valdez Glacier Stream representing the 2012 and 2013 field measurements. Stage represent the water level measurements from the lake.*

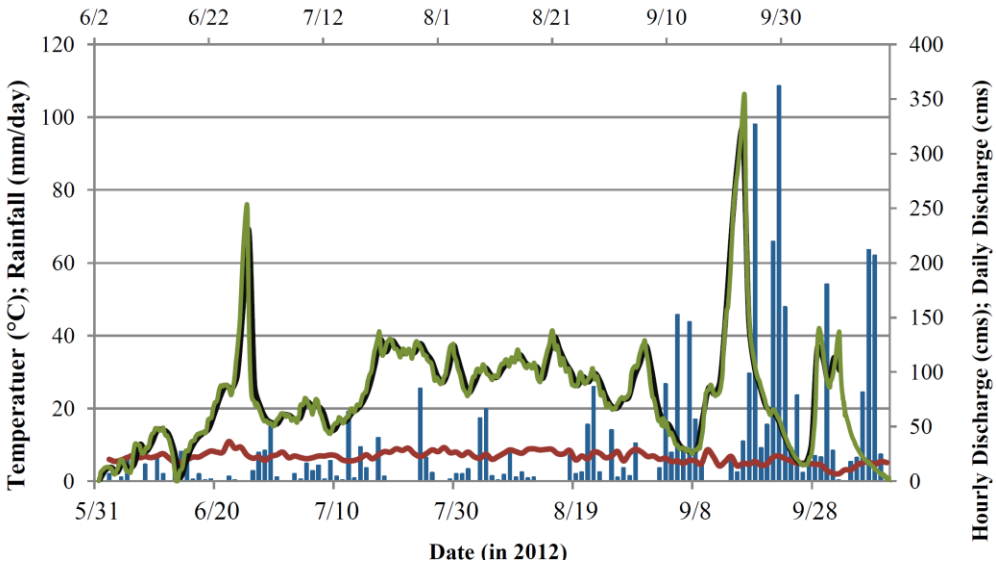

Figure 27. *Estimated mean daily (black) and hourly (green) discharge at the Valdez Glacier Stream during the 2012 melt season, air temperature measured at Valdez Glacier Lake at 77 masl (red) and daily precipitation at Valdez WSO (blue). All flows above 157 cms are a rough estimate.*

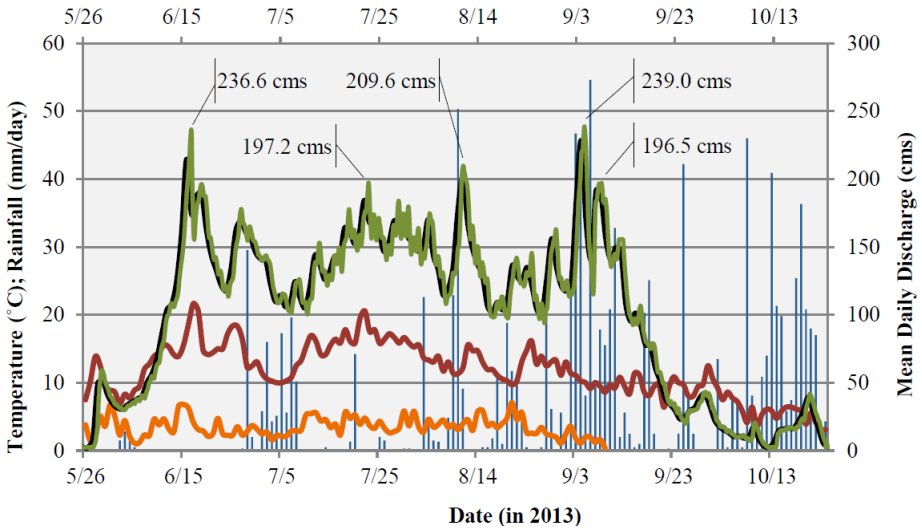

Figure 28. *Estimated mean daily (black) and hourly (green) discharge at the Valdez Glacier Stream during the 2013 melt season, air temperature from Valdez Glacier Lake at 77 masl (red) and from 821 masl (orange) and daily precipitation at Valdez VSO station (blue). All flows above 157 cms are a rough estimate.*

3.2.3 Temperature Index Modeling, Valdez Glacier Stream

A temperature-index model was used to simulate recent summer glacier mass balance and runoff in Valdez Glacier Stream. No future projections were performed. We utilized the Distributed Enhanced Temperature Index Model (DETIM) (Hock, 1999: Hock and Tijm-Reijmer, 2012) due to its application in several studies throughout Alaska. Our field efforts focused on instrumenting

the glacier with temperature and precipitation sensors, which allowed us to calculate a more representative basin-wide temperature and precipitation lapse rate to force model simulations. In addition, we installed an ablation stake network to provide data necessary for calibration of glacier melt. Finally, we initiated stage and discharge observations at the previously un-gauged Valdez Glacier Stream. Streamflow measurements are essential for calibration and validation of the DETIM runoff model.

DETIM is a fully-distributed glacier mass balance model that account for spatial and temporal variability in climate, glacier melt and storage, while routing water through a conceptual linear-reservoir approach (Hock and Tijm-Reijmer, 2012). Glacier ablation is represented by a temperature-index method, which uses air temperature and a melt parameter as a proxy for melt energetics. DETIM calculates melt according to the following equation:

$$M = \left(MF + r_{\frac{snow}{ice}} \times DIRECT\right) \times T, \qquad (3.1)$$

where M is melt, MF is melt factor, $r_{\frac{snow}{ice}}$ is radiation coefficient for snow or ice, DIRECT is direct radiation, and T is air temperature. The linear reservoir approach assigns storage parameters to each of four hydrological units: rock, snow, ice and firn. The rock unit is defined as non-glacierized areas, the snow unit incudes regions on- or off-glacier that are snow-covered and located outside of the firn area and the ice unit includes areas of exposed ice located outside of the firn region (Hock and Tijm-Reijmer, 2012).

Results of air temperature and precipitation from the Precipitation-elevation Regressions on Independent Slopes Model (PRISM), were used to gap-fill missing field measurements for the model calibration. PRISM climatological normals from 1971-2000 (800-m^2 resolution) were used to calculate lapse rates.

Discharge from snow melt dominated contributions to the hydrograph throughout the season (2486 mm, 61%), with the greatest contributions occurring during the spring, and slowly decreasing toward late summer. Firn contributions were elevated starting in late June and extending through mid-September, comprising 1041 mm (26%) of total specific runoff. Discharge from ice peaks in early September, with the total contribution to specific runoff calculated at 362 mm. Runoff from the rock reservoir contributed a total of 169 mm (4%) to total specific runoff. Total annual runoff contributions from Valdez Glacier (i.e. snow, firn, and ice from within the glacier outline) was equal to the summer glacier mass balance (-2.72 m w.eq., or 9.23 x 10^8 m^3). The summer glacier mass balance was approximately 69% of the total annual measured runoff (3.91 m, or 1.33 x 10^9 m^3), or 57% of the total annual modeled runoff (4.79 m, or 1.62 x 10^9 m^3).

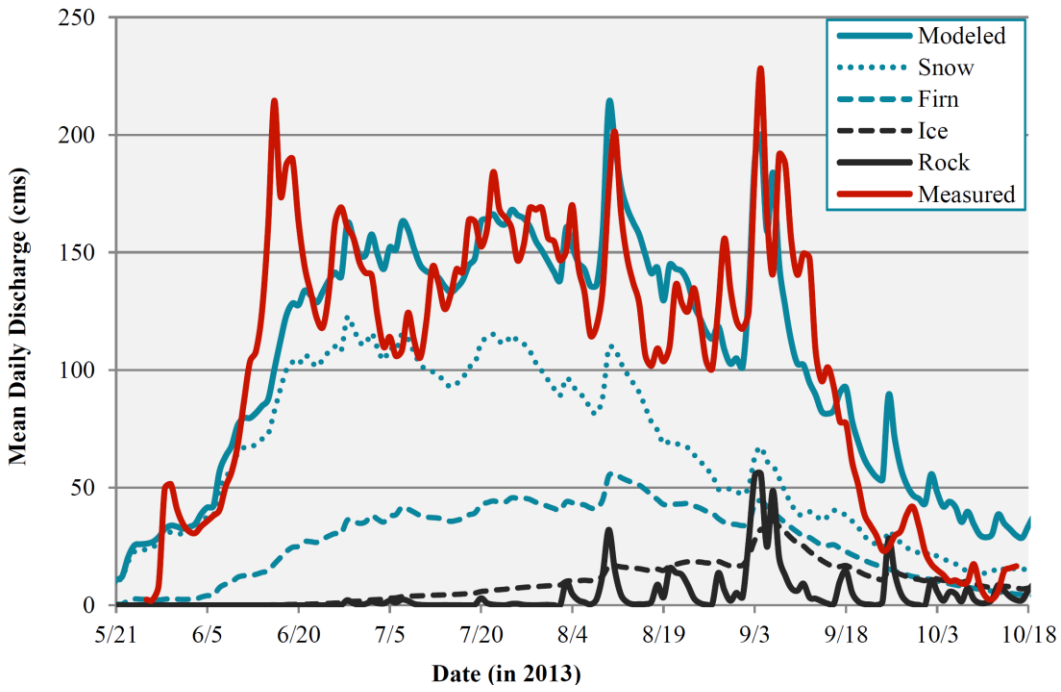

Figure 29. *Measured (red) and simulated (blue) mean daily discharge of Valdez Glacier Stream in 2013 including the portioning of the hydrograph. The "rock" reservoir represents rainfall-derived runoff generated by non-glacierized areas. Note that "measured" estimated discharge above 157 cms are a rough estimate as the stage-discharge relationship was only representative up to 157 cms.*

Table 11. *Simulated total annual specific runoff in 2013 from respective model reservoir (snow, firn, ice and rock/rain) and simulated portioning of the hydrograph during two peak flow events in late summer-early fall.*

Reservoir	Total Specific Runoff from Unit, 2013 (mm)	% of Total Modeled Annual Specific Runoff	% of Total Specific Runoff from Peak Flow Event, August 10	% of Total Specific Runoff from Peak Flow Event, September 4
Snow	2486	61%	58%	38%
Firn	1041	26%	30%	27%
Ice	362	9%	8%	20%
Rock	169	4%	4%	15%

3.3 Phelan Cr.

3.3.1 Temperature Index Modeling, Phelan Cr.

Measured daily air temperature and precipitation (USGS) was used to force the model simulations during the calibration phase (1967-2009). Once the model was calibrated, future projections were forced with a combination between measured air temperature and precipitation and climate projections. Downscaled climate projections (20 km), in which the CCSM3 simulations were

downscaled with fine resolution regional model Arctic MM5, were averaged into three periods: 2000-2009, 2010-2019, 2050-2059 and 2090-2099 (Table 12). The mean air temperature difference between each time slice and the 2000-2009 mean measured temperature was added to the daily 2000-2009 air temperature. Precipitation was assumed to remain unchanged. The simulations do not factor in decreasing glacier area relative to melt. Therefore, the predicted future discharge and glacier mass balance estimates are most likely overestimated. After the dramatic increases in runoff and glacier melt, it is expected that runoff and melt balance will begin to decrease when the glacier area becomes significantly smaller.

Dramatic increases in modeled runoff occurred with each time period (Fig 30) Modeled mean daily, maximum and total discharge increase, while modeled winter, summer and annual glacier mess balance becomes increasingly negative (larger losses). Modeled annual glacier mass balance for time period 2090-2099 is ten times the measured annual mass balance for 2000-2009.

Table 12. *Measured men annual air temperature for 2000-2009 along with values representing the downscaled climate simulations.*

Time slice	2000-2009 (measured)	2010-2019	2050-2059	2090-2099
Mean temperature (C°)	-3.00	-1.01	0.91	2.38

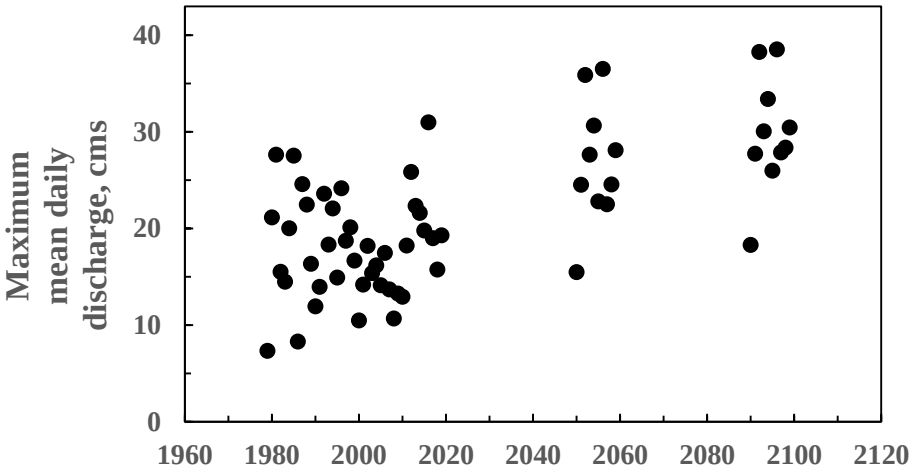

Figure 30. *Projected mean daily annual maximum runoff, Phelan Cr., during selected time periods from 1979 to 2099.*

Table 13. *Modeled mean daily, maximum and total discharge at Phelan Cr. for each time period along with measured mean daily discharge and maximum and total runoff for 2000-2009. All values are in m^3 s^{-1}. Note, these simulations included a static glacier extent, i.e. the glacier was not allowed to shrink.*

Time slice	Mean daily discharge	Maximum discharge	Total discharge
2000-2010 (measured)	2.31	21.41	7,569
2010-2019	3.62	31.02	11,879
2050-2059	5.21	36.54	17,099
2090-2099	6.42	38.56	21,072

Table 14. *Modeled winter summer and annual mass balance, Phelan Cr., for each time period along with measured mass balance for 2000-2009. All values are in* m^{yr-1}*. Note, these simulations included a static glacier extent, i.e. the glacier was not allowed to shrink.*

Time slice	Winter mass balance	Summer mass balance	Annual mass balance
2000-2010 (measured)	1.29	-2.01	-0.72
2010-2019	0.82	-3.33	-2.51
2050-2059	0.20	-5.32	-5.12
2090-2099	-0.40	-6.74	-7.14

3.3.2 Flow frequency analysis, Phelan Cr.

A flow frequency analysis was conducted to examine the frequency of events on the Phelan Creek (Table 15). An analysis was first performed on annual instantaneous (sub-daily) peak flow data from the US Geological Survey Phelan Creek Station (Fig. 31). The analysis was later performed using annual mean daily peak flow data from model simulations (Figures 32-34). The annual peak flow event was not analyzed for its composition, which include glacier melt, snowmelt and/or rainfall. Accordingly, the annual event could be rainfall, glacier- or snowmelt generated, which adds additional uncertainty to the analysis because the data is not considered homogenous. All analyses were completed according to the Interagency Advisory Committee on Water Data, Hydrology Subcommittee, Bulletin 17B (Log Pearson III distribution) using HEC software.

The skew changes from negative to positive from the historical (1979-1999) to future projections (2000-2099) with the skew becoming increasingly positive over time. The mean daily flow at the 1% probability level increase over time from ~35 (2000-2019) to 45 cms (2090-2099). Simultaneously, the 98% probability flow rate increases from ~10 (2000-2019) to 25 cms 2090-2099). It should be noted, however, that the glacier was not allowed to retreat in these model simulations. The static glacier extent result in a bias that overestimate long-term projections in glacier melt under a warming climate scenario as the glacier would otherwise retreat up into higher elevations where air temperatures are cooler. Note that the exceedance probability plot based upon the USGS measurements represents hourly data, while the model projections represent mean daily runoff. The rate of the simulated annual peak flow is a conservative estimate due to the daily averaging.

Table 15. *Simulated mean daily peak flows.*

Analysis	**Period of Record**	**Number of annual events**	**Number of low outliers**	**Station Skew**
1	1979-1999	21	1	-0.951
2	2000-2019	20	0	0.281
3	2050-2059	10	1	0.440
4	2090-2099	10	1	0.633

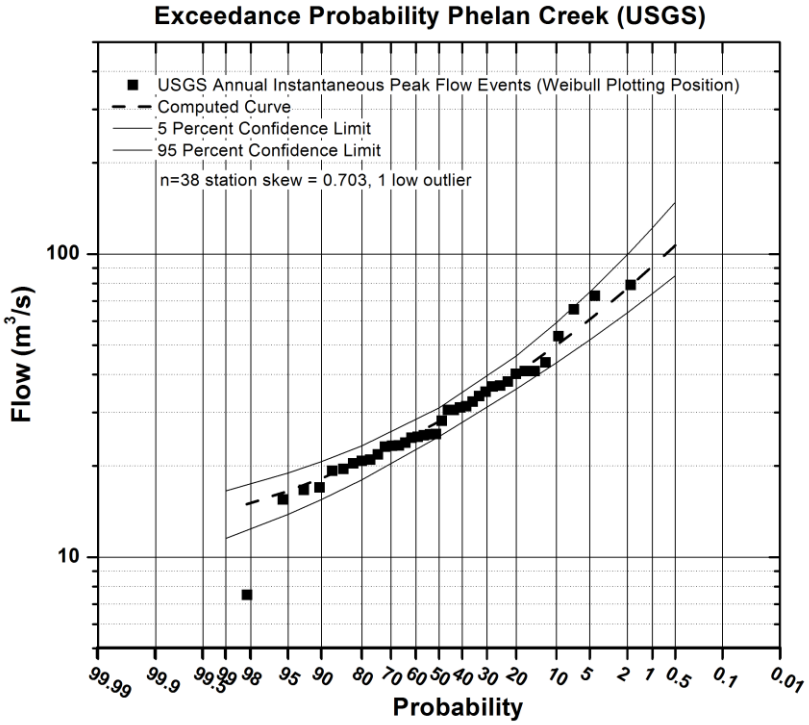

Figure 31. *Exceedance probability at Phelan Cr. based upon measured flows (hourly) in 1967-1979 and 1990-2009.*

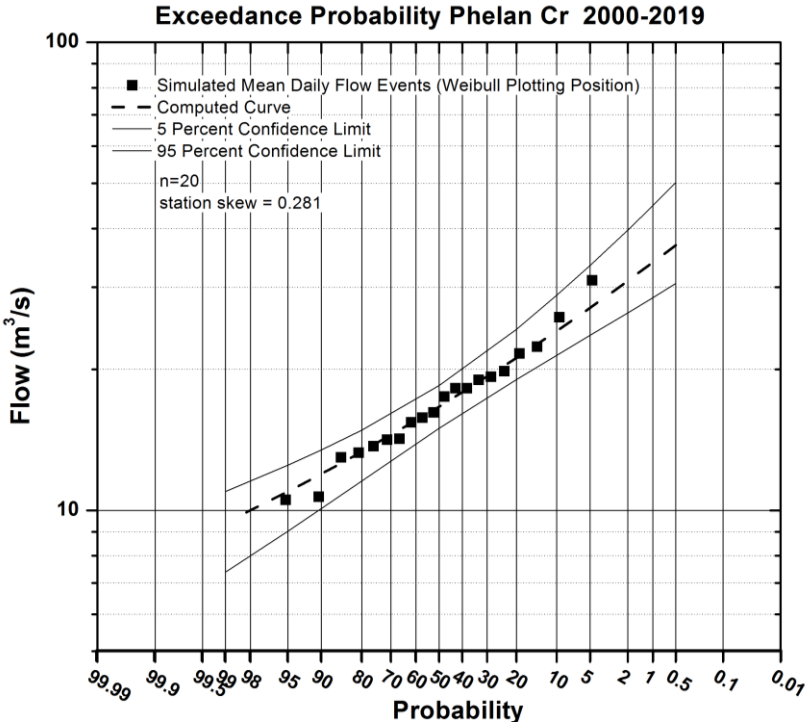

Figure 32. *Exceedance probability at Phelan Creek based upon projected mean daily flows during the period 2000-2019.*

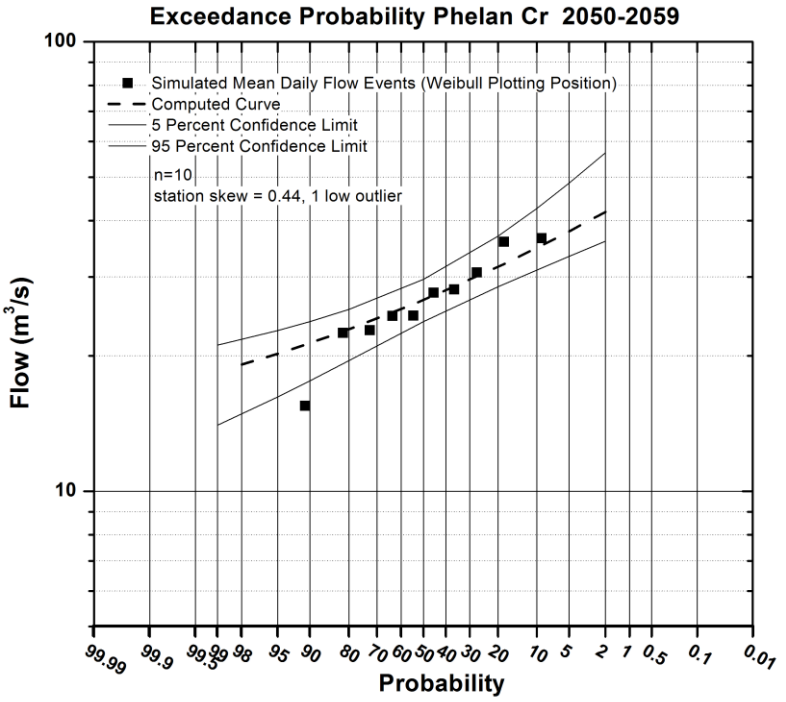

Figure 33. *Exceedance probability at Phelan Creek based upon projected mean daily flows during the period 2050-2059.*

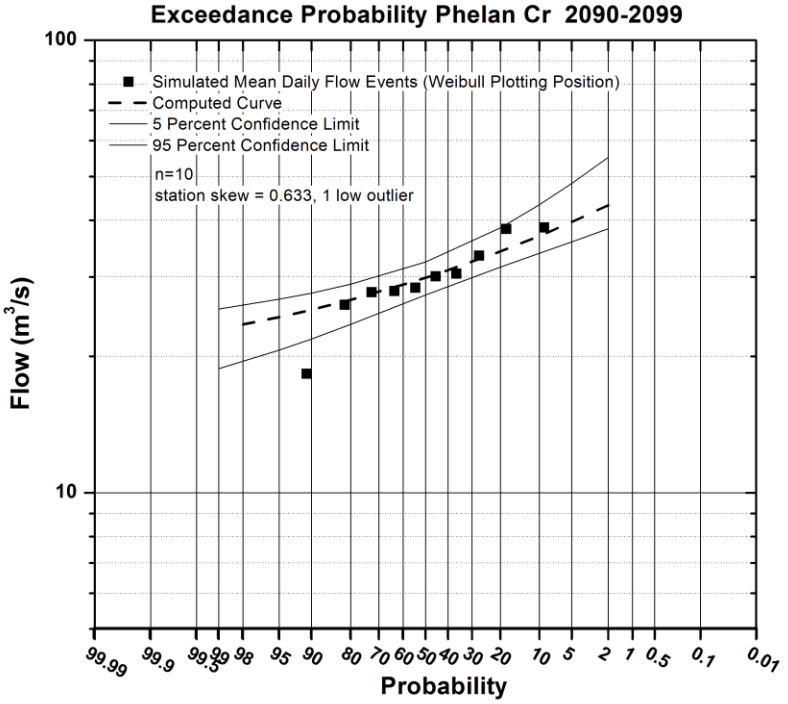

Figure 34. *Exceedance probability at Phelan Creek based upon projected mean daily flows during the period 2090-2099.*

4. Acknowledgements

This work was supported by the Alaska Department of Transportation and Public Facilities, Pacific Northwest Transportation Consortium and through new faculty start-up funding from the Institute of Northern Engineering, University of Alaska Fairbanks.

5. References

Adalgeirsdottir, G, T. Johannesson, H. Bjornsson, F. Palsson and O. Sigurdsson, 2006. Response of Hofsjokull and southern Vatnajokull, Iceland, to climate change, *J. Geophys. Res*., 111, F03001, doi:10.1029/2005JF000388.

Arendt, A., K. Echelmeyer, W. Harrison, C. Lingle, S. Zirnheld, V. Valentine, B. Ritchie, M. Drichenmiller, 2006. Updated estimates of glacier volume changes in the western Chugach Mountains, Alaska, and a comparison of regional extrapolation methods. *J. Geophys. Res.*, 111, doi: 10.1029/2005JF000436.

Hock, R., 1999. A distributed temperature-index ice- and snowmelt modeling including direct solar radiation. J. Glaciology, 45(149), 101-111.

Hock, R., P. Jansson and L. Braun, 2005. Modelling the response of mountain glacier discharge to climate warming. In: Huber, U. M., M. A. Reasoner and H. Bugmann (Eds.): Global Change and Mountain Regions - A State of Knowledge Overview. Springer, Dordrecht, 243–252.

Hock, R. and Tijm-Reimer, 2012. A Mass Balance, Glacier Runoff and Multi-Layer Snow Model: DEBAM and DETIM. 27 pp.

Hodgkins, G.A., 2009. Streamflow changes in Alaska between the cool phase (1947-1976) and the warm phase (1977-2006) of the Pacific Decadal Oscillation: The influence of glaciers, Water Resources Research, 45, W06502, doi: 10.1020/2008WR007575.

Hood, E., and L. Berner, 2009. The effect of changing glacial coverage on the physical and biogeochemical properties of coastal streams in southeastern Alaska. *J. Geophys. Res*., 114, G03001, doi:10.1029/2009JG000971

Neal, E.G., M.T. Walter and C. Coffeen, 2002. Linking the Pacific Decadal Oscillation to seasonal stream discharge patterns in southeast Alaska, *J. Hydrology*, 263, 188-197, doi:10.1016/S0022-1694(02)00058-6.

Neal, E. and Host, R. 1999. Hydrology, geomorphology and flood profiles of the Mendenhall River, Juneau, Alaska. U.S. Geological Survey Water-Resources Investigations Report 99-4150.

O'Neel, S., E. Hood, A, Arendt and L. Sass 2014. Assessing streamflow sensitivity to variations in glacier mass balance. Climatic Change, DOI: 10.1007/s10584-013-1042-7.

Patrick, J. H. and P. E. Black, 1968. Potential evapotranspiration and climate in Alaska by Thornthwaite's classification, USDA Forest Service Paper PNW-71, Juneau, Alaska.

Radić, V. and R. Hock, 2011. Regionally differentiated contribution of mountain glaciers and ice caps to future sea-level rise, *Nature Geoscience*, 4, DOI: 10.1038/NGEO1052.

Rovansek, Ronald J., Larry D. Hinzman, and Douglas L. Kane, 1996. Hydrology of a tundra wetland complex on the Alaskan arctic coastal plain, USA, *Arctic and Alpine Res.,* 311-317.

Schulla, J., 2013. Model Description, WaSiM, Water balance Simulation Model. Zurich.

Tidwell, A., 2010. Impact of climate variability and change on flood frequency analysis for transportation design, Final Report, Prepared for Alaska Department of transportation and Public Facilities and Alaska University Transportation Center, 35 p.